

~~CONFIDENTIAL~~

Copy
RM E54115

6

UNCLASSIFIED



RESEARCH MEMORANDUM

EXPERIMENTAL INVESTIGATION OF CONTROL SIGNALS AND THE
NATURE OF STALL AND SURGE BEHAVIOR
IN A TURBOJET ENGINE

By G. J. Delio and P. M. Stiglic

Lewis Flight Propulsion Laboratory
Cleveland, Ohio

CLASSIFICATION CHANGED

To UNCLASSIFIED

By authority of NACA RA-1 Date 9-17-58
Effectiveness
CLASSIFIED DOCUMENT 958

This material contains information affecting the National Defense of the United States within the meaning of the espionage laws, Title 18, U.S.C., Secs. 793 and 794, the transmission or revelation of which in any manner to an unauthorized person is prohibited by law.

NATIONAL ADVISORY COMMITTEE
FOR AERONAUTICS

WASHINGTON
December 20, 1954

LIBRARY COPY

DEC 22 1954

~~CONFIDENTIAL~~
UNCLASSIFIED

LANGLEY AERONAUTICAL LABORATORY
LIBRARY, NACA
LANGLEY FIELD, VIRGINIA

NACA RM E54115

NATIONAL ADVISORY COMMITTEE FOR AERONAUTICS

RESEARCH MEMORANDUMEXPERIMENTAL INVESTIGATION OF CONTROL SIGNALS AND THE NATURE
OF STALL AND SURGE BEHAVIOR IN A TURBOJET ENGINE

By G. J. Delio and P. M. Stiglic

SUMMARY

An axial-flow turbojet engine was operated on a sea-level static test stand to determine whether or not detectable signals were present in pressures and blade stresses that are usable as stall warnings in control applications. Surge and stall behavior were closely examined for unique characteristics that could be used to control engine behavior in the vicinity of surge and stall. The possibility of optimizing engine acceleration by proper fuel flow manipulation was also studied.

A signal usable as a stall warning appeared in both compressor-discharge pressure and blade stresses only in the narrow range between 65.4 and 73.0 percent rated speed. Surge frequencies were found to be dependent on both fuel flow and engine speed; stall frequencies were found to be dependent only on speed. In the midspeed range the limiting value of compressor pressure ratio appeared to be single valued and continuous when determined for both surge and stall. Engine responses did not lend themselves readily to the optimizing technique tried in this investigation because of the abrupt changes in pressures at stall, hysteresis effects associated with stall, and lags in combustion.

INTRODUCTION

During certain aircraft maneuvers there is a need for rapid thrust changes. The aircraft may use turbojet engines with fixed exhaust-nozzle area and produce thrust changes by changing the engine speed. Thus the need for rapid thrust changes becomes equivalent to a need for rapid engine accelerations. The proper control of acceleration is an important function of turbojet-engine controls. The control must manipulate fuel flow to accelerate engine masses which are high in comparison with the maximum excess torque available. This low torque-to-inertia ratio causes turbojet-engine acceleration to be very sluggish as contrasted to piston-type engines. This is especially true in the range of low turbojet-engine speeds.

For rapid engine acceleration the turbine-inlet temperature or engine pressure ratio should be rapidly increased to the maximum permissible value and maintained at this value during the remainder of the acceleration. During acceleration most controls vary the fuel flow corresponding to the gradually increasing engine speed in such a manner as to avoid compressor damage due to stall, reductions in acceleration, excessive temperatures, and so forth. Most acceleration controls, at present, use schedules (e.g., during acceleration, fuel flow could be increased until compressor-discharge total pressure reached the limiting value represented by a scheduled compressor-discharge total-pressure - speed relation). The difficulties with the application of schedules are changes in the fuel flow limit due to the variability of engines, engine deterioration, inlet-air distortion, and the necessity of complex generators to produce the schedules. Because of these difficulties, only a small part of the acceleration margin (difference in compressor-discharge total pressure between the steady-state pressure and the pressure at stall or surge) is usually used.

A closed-loop control operating on a signal that is uniquely identifiable when the fuel flow is only slightly less than that required to cause stall and surge, and which does not require a calibration, would eliminate the necessity of using schedule controls. Pressure fluctuations have been observed which were associated with stall and surge that offer possibilities of having unique properties at the verge of surge and stall. These properties might be detected as specific-weight-flow fluctuations on hot-wire anemometers, pressure fluctuations in pressure transducers, or as vibratory stresses in stator blades.

The purpose of the investigation described herein is to survey pressure transients and blade-stress phenomena to determine whether or not a detectable signal that indicates stall and surge are impending exists in a modern turbojet engine. Such a signal could be used in a control that would, upon command to accelerate the engine, increase the fuel flow rapidly until the characteristic signal warned of the proximity to stall and surge, then would manipulate the fuel flow to maintain this signal.

Surveys were made of total-pressure fluctuations and stator-blade stresses. The amplitude and frequencies of these quantities were examined to determine whether a characteristic signal was present at the verge of stall and surge. During the experiments other phenomena incidental to the objective but very significant to control designers (such as surge and stall behavior, combustion lag, screech, and partial blow-out) were observed and are reported.

The occurrence of severe hysteresis (associated with stall, ref. 1) and dead time (associated with combustion, ref. 2) complicates the problem of an acceleration control based upon the detection of any characteristic signal that is emitted while the engine is on the verge of stall

or surge. On the other hand, a signal emitted at fuel flows materially less than that required to stall or surge the engine would either result in the control setting a slow acceleration or would necessitate an amplitude calibration of the signal.

In an optimizing-type acceleration control that maintained maximum pressure ratio during acceleration, maximum acceleration need not result because the maximum pressure is a limit only insofar as pressure is concerned. Whereas one engine had coincident maximum pressure ratio and maximum acceleration (ref. 3), another achieved maximum acceleration at pressure ratios lower than those at stall (ref. 4). The existence of partial stall during acceleration could also be damaging.

DEFINITION OF SURGE AND STALL

For this report, surge and stall are defined from material presented in references 5 and 6. Observations of stall in axial-flow compressors have demonstrated that regions of separated or reversed flow occur in more or less well defined regions around the circumference of the compressor annulus and that these regions pass through the compressor in an axial direction with very little spiral motion. The retarded-flow regions are propagated circumferentially with a velocity that is a fraction of the engine speed.

Two principal types of stall exist (fig. 1): partial stall, which is usually tolerated insofar as compressor performance is concerned, especially in the range of low engine speed; and stall (commonly referred to as hard, complete, or full), which must be avoided. (All symbols are defined in appendix A.)

The stall characteristics are:

- (1) Only one region exists; it propagates regularly.
- (2) The region extends over the full blade height.
- (3) The transition into stall is abrupt.
- (4) There is a hysteresis loop.
- (5) The circumferential extent of the stall region increases with decreasing weight flow.

The partial-stall characteristics are:

- (1) It is usually multiregioned.

(2) The regions extend over only part of the blade height and are of varying amplitude throughout the stages.

(3) The transition into partial stall is gradual.

(4) The partial-stall regions regroup into a single region during transition into stall.

(5) At constant speed it occurs at weight flows higher than those of stall.

Surge is defined as weight flow fluctuations which are axially symmetric as compared with weight flow fluctuations of stall caused by low-flow regions revolving about the compressor axis. That is, net flow through the annulus does not vary with time in the case of stall; whereas net flow through the annulus does vary with time in the case of surge. At the lowest weight flow during the surge pulse, the single stall region is spread out to cover the complete compressor annulus (ref. 7).

APPARATUS AND INSTRUMENTATION

The engine (fig. 2) consisted of a 12-stage compressor, an eight-can combustor, a single-stage turbine, and a fixed exhaust-nozzle area. The rated thrust of 5300 pounds at 7950 rpm was produced with an air flow of 98 pounds per second and a fuel flow of 5800 pounds per hour. The compressor pressure ratio was 5.3, and the exhaust-nozzle area was adjusted to produce a rated turbine-discharge temperature of 1275° F at rated speed.

All pressure measurements about the compressor and the turbine discharge were made by pressure probes axially aligned along the top. At the compressor discharge, an additional probe was installed diametrically opposite. In addition, large- and small-slot fuel pressure measurements were made at the nozzles. Fuel-valve position and engine speed were also recorded.

In order to permit momentary excursions into the stall and surge zones by the use of controlled pulses of fuel flow, an entirely new fuel system and fuel control were designed and used. The resulting engine transients of short duration were recorded on an extended-time basis with instrumentation possessing accuracy and precision somewhat greater than that normally used. Both the instrumentation and the fuel system are described in appendixes B and C, respectively.

METHOD AND PROCEDURE

For this investigation, an axial-flow turbojet engine was installed on a sea-level, static test stand. The engine was operated at steady-state conditions throughout the speed range to gather information concerning signals, or noise, present during steady-state operation. Signals usable in an acceleration control must appear above this background. The engine was subjected to different types of acceleration by the proper manipulation of fuel flow so that engine behavior during acceleration and also the feasibility of using some form of an optimizing acceleration control which could accelerate the engine in the shortest possible time could be studied.

Steady-State Survey

The engine was operated at steady-state conditions at specific points throughout the speed range. At each steady-state speed, continuous records were obtained of the total pressures at the compressor inlet and the 1st, 3rd, 5th, 7th, 9th, 11th, and discharge stages. Simultaneously, stator-blade stresses were recorded at the 4th, 7th, and 10th stages.

The frequency response of the compressor- and turbine-discharge total pressures to fuel flow was studied to determine the dynamic characteristics and to aid in the selection of a perturbation frequency for use in an optimizing control. At an engine speed of 69.2 percent rated, fuel flow was cycled at frequencies up to 100 cycles per second with the following variables being recorded: throttle position, throttle-discharge fuel pressure, engine small-slot fuel pressure, compressor-discharge total pressure, and turbine-discharge total pressure.

Acceleration Survey

Step changes in fuel flow were impressed upon the engine in the following sequence: At 37.7 percent rated speed, the step change in fuel flow was sufficiently small to cause an initially small departure from steady-state conditions. Successive steps of increasing magnitudes were applied at the initial speed of 37.7 percent rated until the capacity of the fuel system had been reached. This procedure was repeated at 5-percent-rpm intervals up to $N = 83.0$ percent.

At selected speeds between 46.5 and 75.5 percent rated, ramp changes with superimposed sine waves in fuel flow were impressed upon the engine. The superimposed frequencies varied between 5 and 10 cycles per second.

For both the step and ramp changes in fuel flow, continuous recordings were obtained for the following variables: compressor-discharge total pressure, turbine-discharge total pressure, throttle position, engine speed, small-slot fuel pressure, and the fuel pressure at the throttle discharge. In order to obtain information during these excursions into the stall and surge regions, temperatures higher than the steady-state rated temperature were permitted for not more than 2 seconds, because of the consideration given to strength and durability of the engine parts. All accelerations were permitted to continue until one of the following phenomena occurred: rated turbine-discharge temperature, stall, surge, screech, or partial blow-out.

RESULTS AND DISCUSSION

The search for unique engine characteristics usable as pre-stall warnings has led to varied results, most of which are significant to control designers. These results are presented in three parts:

- (1) A steady-state survey of total pressures and stator-blade stresses are reviewed for indications of the nature of stall and surge build-up.
- (2) An acceleration survey of compressor behavior upon entering into and returning from the stall region is examined with a view towards detecting stall and surge warnings.
- (3) Results of an optimizing signal (ref. 8) are studied for possible application to an acceleration control.

Steady-State Survey

Pressures. - The nature of pressure fluctuations measured simultaneously at different points of the compressor are illustrated in the sample trace of figure 3(a). At an engine speed N of 67.6 percent rated, the oscillating pressures fluctuated regularly; at $N = 68.4$ percent rated, the amplitude was greatly reduced and the fluctuations became somewhat irregular. The variation of the amplitude throughout the speed range is shown in figure 3(b), where it is shown that all magnitudes greatly diminished at 68.0 percent rated speed. The magnitude of the total-pressure variation in the 7th compressor stage changed from 2.7 to 5.6 percent absolute compressor-discharge total pressure as the engine speed varied from 37.7 to 68.0 percent rated; and the absolute value varied from 1/2 to 2 pounds per square inch. This pressure fluctuation dropped to 0.50 percent at 73.0 percent rated speed and increased to slightly more than 1 percent at rated speed.

From an examination of the frequency of these fluctuations, the results shown in figure 4 were obtained. Although the magnitudes of the fluctuations experienced an abrupt reduction at 68.0 percent rated speed, the frequency maintained its linear relation with engine speed. It is suggested that the engine during steady-state operation experienced partial stall in the speed range from $N = 50$ to $N = 88.0$ percent rated, based on the definitions presented earlier. In this range two partial-stall zones existed and the slope (0.85 cycle per rotor revolution) is the propagation rate. At 68.0 percent rated speed, the amplitude of the partial-stall zone quickly reduced with increasing speed. Below 44.0 percent rated speed, the increased frequency indicated more than two partial-stall zones, and the line drawn through the data points would be for three stall zones at the same propagation rate.

Stator-blade stresses. - An examination of stator-blade stresses during the preceding pressure fluctuations, which occurred during steady-state operation, showed marked changes in blade loading and vibratory stresses (fig. 5). The mean line is indicative of blade loading, and the shaded area is indicative of the stress vibrational amplitude. The strain gages were so oriented as to include as much of the bending stress as possible. Over the speed range investigated, no resonance peaks were observed.

Vibratory stress in the 4th stator stage (fig. 5(a)) increased with speed to approximately $N = 40.0$ percent rated and remained at this amplitude to 68.0 percent. Blade loading, indicated by the average stress, was light for speeds below 44.0 percent rated. At this speed there appeared a marked change in the flow pattern. The speed at which the partial-stall amplitude abruptly diminished ($N = 68.0$ percent rated in fig. 3(b)) appeared to coincide with the speed at which there was a marked decrease of vibrational stress; also, the speed at which there was a transition from multiregion to two-region partial stall ($N = 44.0$ percent rated in fig. 4) appeared to coincide with the speed at which the blade loadings reversed (fig. 5). The recorded amplitudes of the stresses in figures 5(b) and (c) were attenuated because of the frequency-response limitations of the stress recorders. From figure 5 it is deduced that partial stall served as the aerodynamic excitation. The resulting vibratory blade stresses might serve as a signal for stall sensing, but this would be difficult because of resonance peaks connected with the blade natural frequencies.

Frequency response. - The total-pressure responses at the compressor discharge and the turbine discharge to sinusoidally varying fuel flow at a constant average speed is presented in figure 6. Resonance peaks were found in the turbine-discharge total-pressure response (points A, B, C, and D) and they were thought to be caused by the large volumes present in the engine, such as combustors, tail pipe, diffuser, and so forth. No such peaks were found in the compressor-discharge

total-pressure response below that frequency at which actual fuel flow attenuated. The one peak in the compressor-discharge total-pressure response (point E) could be attributed to some receiver volume at the compressor discharge. The cavity resonances, points A and B, could be connected with surge behavior.

The compressor-discharge pressure response "fell-off" at about 20 cycles per second, whereas the turbine-discharge total-pressure response followed fuel flow variations to higher frequencies. This indicated that a portion of the burning occurred in the tail pipe for frequencies above 20 cycles per second. This corner frequency of 20 cycles per second can be considered an approximation of that part of the combustion lag due to burning. That is, pressure due to combustion increased exponentially in a characteristic time of 8 milliseconds. Further contributions to combustion delay are shown in the following section.

Acceleration Survey

Fuel flow was manipulated during engine acceleration in the manner shown in figure 7. The different types of engine behavior which resulted from testing for the compressor-discharge total-pressure limit produced engine phenomena which must be considered in control design. Typical engine acceleration responses are shown in figure 8. In figure 8(a), the fuel flow change was less than that required to reach the limiting pressure, and the resulting acceleration was less than the realizable maximum. The fuel flow change was delayed by the transport time required between the throttle and the nozzles. Additional delay was apparent between the fuel flow at the nozzles and the response in compressor-discharge total pressure. The total delay was of the order of 30 milliseconds. The condition of partial stall (defined earlier) existed throughout the acceleration. Other data indicated that the partial-stall magnitude varied with speed in a quasi-steady-state manner, reproducing even the abrupt magnitude change as engine speed changed from 62.8 to 73.0 percent rated (see fig. 3(b)). However, there occurred no abrupt changes in effective discharge pressures during acceleration.

In figure 8(b), the fuel flow change was sufficient to skirt and then reach a limiting pressure. This limiting pressure at the instant of stall, and instantaneous speed, is called the critical pressure. During the initial phase of the acceleration, the magnitude of partial stall increased. At the instant critical pressure was reached, there was a transition from partial stall to stall, as defined previously. The transition was practically instantaneous, and effective pressure was reduced.

The stall region was a localized area of reduced, or reversed, air flow rotating at a fraction of engine speed. As seen by the total-pressure probe, the fluctuations were caused by first a stalled zone,

then an unstalled zone passing the probe. The data indicate that the stall region was smaller than the unstalled region; thus, less than half the annulus was stalled.

As the region of retarded air flow rotated about the engine axis, with the fuel flow being held constant, there occurred a periodic enriching of the fuel-air ratio in each burner at the frequency of stall. This frequency prompted post-turbine burning, as was indicated in the section on frequency survey. However, alternate enriching is a secondary point. Stall was indicated by reductions in average compressor-discharge total pressure, turbine-discharge total pressure, and acceleration, probably caused by a mean reduction in mass flow. Alternate enriching may have caused average pressures and acceleration to be lower than otherwise.

Although fuel flow was rapidly reduced, the compressor was not immediately affected and required time to recover to normal air flow conditions. During recovery, the circumferential extent of the stall region diminished and disappeared, and hence net air flow increased. This hysteresis effect, characterized by the recovery time, existed for a time greatly in excess of that needed for the flow pattern to be re-established about cascaded airfoils. When fuel flow was cut back, the compressor-discharge total pressure did not drop sufficiently to allow the compressor to come out of stall and the air flow to increase. The pressure was maintained momentarily by either the burning process progressing upstream to the fuel nozzles or the heat storage effect of the engine or both. During this time, partial blow-out was corrected. The recovery time (0.2 sec on the average) exaggerated the hysteresis effect.

In figure 8(c), the fuel flow change was more than sufficient to cause the compressor-discharge total pressure to reach critical pressure. When critical pressure was reached the first time, the single stall region probably spread out to cover the complete compressor annulus and initiated the surge pulse, as defined previously. The total pressure dropped to a sufficiently low value to allow the compressor to recover and subsequently to return again to the critical pressure. In this manner one cycle of surge was completed.

The engine accelerated during surge until only part of the annulus was stalled and conditions were fulfilled as described for stall behavior. Under these conditions, the mixture did not burn completely until it reached the tail cone. For the increase in fuel flow shown in figure 8(c), partial blow-out occurred after an apparent steady condition was reached (perhaps one or more burners experienced rich blow-out), and the pressure fluctuations evident in stall now occurred in the turbine-discharge total pressure. The average acceleration decrease was caused by (1) post-turbine burning raising the average turbine-discharge pressure, and (2) a possible nonlinear effect of oscillating turbine-discharge

pressure on average acceleration. Although the acceleration recorded on figure 8(b) indicated that the turbine-discharge total pressure dropped at the instant of stall, that on figure 8(c) indicated that the turbine-discharge total pressure rose at the instant of partial blow-out. The latter figure also indicated that combustion "filtered" or averaged the fluctuations in compressor-discharge total pressure due to a stalled compressor.

Surge resulting from an increased step change in fuel flow is shown in figure 8(d). The compressor-discharge total pressure quickly reached critical pressure, at which point the entire discharge annulus was probably stalled. This was followed by a drop in pressure, allowing the compressor to recover to the critical pressure a second time. The repeated recovery to critical pressure (alternate complete stalling and unstalling of the compressor) characterized surge, and the accompanying change in net flow through the compressor at surge frequency was reflected in the in-phase variation in turbine-discharge total pressure. In contrast (fig. 8(b)), stalled operation produced no fluctuation in the turbine-discharge total pressure. There was different filtering action in the combustors at the frequency of stall than at the frequency of surge. During stall, the space average of the flow, or net flow, was essentially constant in time in the combustors; whereas during surge, this space average fluctuated in time at the surge frequency.

The large increase in fuel flow which surged the engine (fig. 8(d)) produced pressure fluctuations so large that, when fuel flow was returned to the initial value, time was required to attenuate the surge cycles. During this time, the compressor was also stalled. This indicated that surge is a function of the compressor environment, whereas stall is a function of the compressor alone (ref. 7).

An acceleration resulting from extreme increases in fuel flow was recorded on figure 8(e). In this low-speed range ($N = 42.0$ percent rated), excessive fuel flow caused a sudden change in turbine-discharge total pressure which indicated a drop in burner efficiency and an increase in post-turbine burning. The unburned fuel in the tail cone caused post-turbine burning and subsequent screech. Partial blow-out and screech had negligible effect on compressor-discharge total pressure, which indicated that, in the low-speed region, compressor-discharge total pressure could not be used as a sensor for the detection of partial blow-out and screech.

Stall behavior. - The instantaneous values of the total pressures in a stalled compressor are recorded on figure 9. Each of the total-pressure probes in the first six stator stages was aligned axially with the upper compressor-discharge total-pressure probe. The phase relation of these pressures indicated that a pressure sensor, to be used for stall detection, can be located anywhere in the compressor. The stall

region extended axially throughout the compressor and propagated at a fraction of engine speed. The two total-pressure probes (P_{12a} and P_{12b}) at the compressor discharge were diametrically opposed, and the pressures they recorded were 180° out of phase. The extremely small elapsed time involved in the transmission of the signal through the compressor (or perhaps the fact that all stages stall) makes the determination of which stage initiates stall extremely difficult. Thus instrumenting the critical stage and detecting stall in it before stall spreads throughout the rest of the compressor would be very difficult.

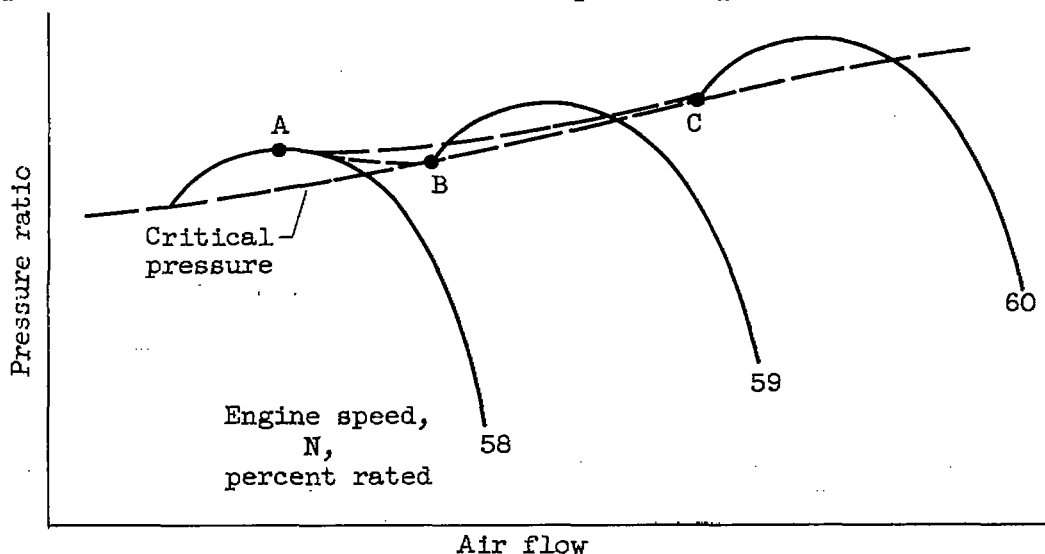
The dependence of stall frequency on speed is illustrated in figure 10: Its slope, or propagation rate (0.43 cycle per engine revolution, from 40 to 80 percent rated engine speed), for one stalled zone correlated with the propagation rate for two partial-stall zones (fig. 4). Thus, a stall sensor based on the propagation characteristics of stall might be used to limit fuel flow. This sensor could incorporate a band-pass filter which permitted only information pertaining to stall to be sensed (e.g., fig. 8(b), 43 cps at $N = 67.8$ percent rated).

The critical pressure and the amplitude of stall for every point in the speed range are plotted in figure 11(a). The limiting pressure is commonly used as a schedule in control systems to limit fuel flow during acceleration. In the speed region below 53.0 percent rated, the critical pressure coincided with the peak compressor-discharge total pressure once during every cycle of fluctuation in stall. Above 53.0 percent rated speed, the compressor-discharge total pressure never recovered to the critical pressure once the engine had stalled. Only in this speed region did the engine surge. The frequency and the amplitude of stall appeared independent of fuel flow beyond that required for stall and of the rate of increase in fuel flow.

The average, or effective, pressure during stall increased linearly with engine speed but was always below the critical pressure. The percentage pressure loss is given in figure 11(b). When the pressure loss exceeded 16 percent of the pressure rise across the compressor, the engine could surge.

The effect of excessive fuel increases on compressor-discharge total-pressure ratio during acceleration is illustrated in figure 12(a). At 58.0 percent rated speed, several excursions were made into the stall region with increasing amounts of added fuel flow. When the fuel flow was increased suddenly to 4550 pounds per hour, the compressor-discharge total pressure immediately exceeded the critical pressure, then increased with speed at constant fuel flow to the critical pressure where the conditions for stall were fulfilled. For larger increases in fuel flow, the critical pressure was reached sooner and at lower speeds. This behavior could be explained by postulating the air flow characteristics

for this compressor as illustrated in the following sketch. Multistage compressors have been tested that have pressure peaks at air flows higher



than those necessary for stall (ref. 7) in this speed range. Thus the acceleration at a fuel flow of 4550 pounds per hour (fig. 12(a)) could follow the path AC, and the accelerations at higher fuel flow could follow the path AB.

For increasingly higher initial engine speeds (fig. 12(b)), the compressor-discharge total pressures in response to step changes in fuel flow exceeded the critical pressures to a corresponding lower degree (i.e., the slopes of the constant-speed lines increased, and the critical-pressure point approached the maximum pressure). When critical pressure was reached, the pressure instantly dropped and fluctuated at the stall frequency (fig. 10) and about the average stalled pressure. The average pressure line during stall indicated that the compressor is an inefficient pressure generator but could still generate sufficiently to accelerate the engine (fig. 8(b)).

Schedule difficulties. - The exceeding of the critical pressure following a burst of fuel, especially in the low-speed range, can make the use of schedules difficult (e.g., limiting fuel flow during acceleration according to the maximum value of compressor-discharge total pressure at a certain speed). The control must depend on the schedule to determine which limit to place on fuel flow. This limit, according to figure 12(a), can be between 4500 and 5300 pounds per hour at an engine speed of 58.0 percent rated, depending on the manner in which the control wishes to approach critical pressure. The engine operating point is multivalued with respect to compressor-discharge total pressure, and the compressor-discharge total-pressure - engine speed limit is likewise multivalued.

A fuel flow - engine speed schedule obtained by plotting similar transients in this speed range is shown to be single valued (fig. 12(c)) (i.e., the control could schedule only one maximum fuel flow to avoid stall and surge). The approach to the limiting value from inside the curve is caused by combustion lag. Above 68 percent rated speed, either the compressor-discharge total-pressure - engine speed or the fuel flow - engine speed W-N schedule would be applicable. The existence of the minimum value in the limit curve shown in figure 12(c) correlates with the behaviors shown in figures 3 and 4, where the blade stresses and pressure fluctuations show marked changes in air flow behavior at 68 percent rated speed.

Surge behavior. - The behavior of the compressor-discharge total pressure during accelerations into the surge region is illustrated in figure 13. In figure 13(a) the pressure ratio across the compressor is related to engine speed during two particular accelerations starting at $N = 72.8$ and $N = 78.0$ percent rated. The surge pulse was initiated by a general breakdown of flow at the instant critical pressure was reached; that is, the entire compressor annulus was stalled. At this instant, acceleration was maximum. During the negative part of the cycle, the discharge total pressure dropped to a value sufficient for the compressor to recover and to again reach the critical pressure. In this manner, the positive peaks of the surge cycles always reached the critical pressure.

The critical pressure obtained at 67.8 percent rated speed (fig. 8(b)) at the instant of stall and the critical pressure obtained at 65.5 percent rated speed (fig. 8(c)) at the instant of surge are plotted on the same critical-pressure line in figure 11(a). The critical-pressure line was extrapolated at the higher-speed end by using the successive pressure peaks of surge during acceleration (e.g., fig. 8(d)). In the intermediate-speed range, the pressure peaks at stall and the pressure at the instant of stall yielded the same critical pressure. Surge appeared insensitive to the rate of increase in fuel flow.

At the low speeds, the surged phase lasted for one or less cycles of surge (fig. 8(c)) and the transition into stall occurred at constant fuel flow. At the higher speeds (fig. 8(d)), where the pressure loss at stall was greater, surge continued with increasing amplitude. This was caused by positive engine acceleration which progressively raised the critical pressure, and the engine continued to surge because the pressure loss (fig. 11(b)) increased with speed.

The surge frequency obtained by step changes in fuel flow (barely sufficient to cause surge) is given in figure 13(b) for different initial speeds. The frequency decreased with increasing engine speed, possibly because of increasing weight flow. The surge frequency obtained at constant speed, but with progressively larger step changes in fuel

flow, is given in figure 13(c). For this case, the frequency increased with increasing fuel flow, possibly because of a stiffer spring rate (i.e., higher pressure resulting from the increasing fuel flow). The lower frequencies for 78.0 percent rated speed may again be caused by the higher weight flow.

Stall warnings. - The only indication of approaching stall or surge during an acceleration attempt was found in the speed range from 65.4 to 73.0 percent rated. A recording of blade stresses (fig. 14(a)) indicated a build-up of partial-stall amplitude, with the frequency and phase coinciding with total-pressure fluctuations, immediately prior to surge. There was an abrupt transition into surge, followed by stall. The blade stresses indicated not only the blade-loading effect resulting from increasing weight flow with increasing speed, but also the magnitude of stress change due to surge and stall. Thus partial stall, together with stall and surge, served as aerodynamic excitation for blade vibration. As a result, it may be possible to use stator-blade stresses as a stall sensor. However, this engine operated under conditions of partial stall even in steady-state operation, and a stall sensor based on the increasing amplitude of partial stall to serve as a warning of approaching stall and surge would have to be calibrated for amplitude as well as frequency.

A closer examination of total pressures (fig. 14(b)) indicated that stall warnings could be sensed throughout the compressor. The 2nd, 5th, and discharge stages of the compressor showed corresponding increases in the magnitude of partial stall (which has been shown to exist in steady-state operation) near the critical-pressure value. The increase in magnitude of the total-pressure fluctuations, which has a frequency of 0.85 percent rated speed, could serve as a stall warning. These warnings appeared in response to step changes in fuel flow. Figure 14(c) indicates that this type of stall warning resulted as well from ramp changes in fuel flow even though the engine started at an initial speed where partial-stall amplitude was greatest (fig. 3(b)). This figure also shows a progressive increase in amplitude of partial stall with fuel flow increases, which again shows the need for amplitude calibration.

Investigation of an Optimizing Technique

The saturation effect in pressure response to increasing fuel flow is shown in figure 15. The deviation from a linear relation could be caused by the "flattening out" of the air flow of the compressor with increasing pressure, and the decreasing efficiency of the combustors with increasing fuel flow. Using peak pressure as coincident with maximum acceleration, as found for this engine (ref. 3), an optimizing acceleration control based on pressure could produce the fastest acceleration. The optimizing acceleration control utilizing the principles

of reference 8 would superimpose a sinusoidal variation of relatively small amplitude on the input, would measure the resulting amplitude and phase in the output, would compare these with the input, and would use the comparison to approach the optimum point by manipulating fuel flow during the process of adjusting for optimum acceleration.

Fuel flow inputs which simulate a type of optimizing-control behavior were impressed on the engine. These inputs, ramp changes with superimposed sinusoidal variations in fuel flow, produced effects in engine speed and compressor- and turbine-discharge total pressures as recorded on figure 16. At a speed of 46.6 percent rated (fig. 16(a)), the response of compressor-discharge total pressure indicated an approach to an optimum pressure. The amplitude of the fundamental frequency approached zero at critical pressure, and the slope of the speed trace increased as the compressor-discharge total-pressure signal decreased until, at zero signal, the acceleration was maximum. The amplitude of partial stall increased as critical pressure was reached. However, after critical pressure had been reached and the compressor had stalled, the oscillating fuel flow had much less effect on the compressor behavior. The average fuel flow continued to increase during stall until partial blow-out occurred. The phase difference between indicated fuel flow (throttle position λ) and compressor-discharge total pressure was a measure of total combustion lag (approx. 35 milliseconds).

At 56.6 percent rated speed (fig. 16(b)), attenuation of compressor-discharge total-pressure response still appeared but did not reach 100 percent. This was the effect of the higher initial speed. As the pulsating fuel flow probed closer to the critical pressure, the magnitude of partial stall increased; and when critical pressure was reached the first time, the transition point into stall had been reached. At this time, a cycle of low pressure occurred with a superimposed partial-stall signal having a frequency of 0.85 percent rated engine speed that had been present before at a much lower amplitude. However, the decreasing phase of the cycling fuel flow prolonged the transition and allowed the critical pressure to be reached a second time. Because this peak in fuel flow was slightly higher than the previous one (due to ramp change), the compressor stalled. A fast control capable of varying fuel flow during this transition time of approximately 0.1 second could possibly have prevented stall.

At 61.7 percent rated speed (fig. 16(c)), the attenuation of the compressor-discharge total-pressure response was diminished as critical pressure was approached. Thus, attenuation decreased as the initial speed of each acceleration attempt was increased. Here, again, the transition into stall was prolonged, which indicates a possibility for a fast control to skirt the stall zone. The critical pressure was almost reached at the positive peaks of the following few cycles of fuel flow. The cycling fuel flow continued to modulate the average compressor-discharge total pressure during stall.

At an engine speed of 72.7 percent rated (fig. 16(d)), a speed at which transition into stall is always accompanied by a large drop in compressor-discharge total pressure, the attenuation in pressure is fairly low. Thus, an amplitude calibration of pressure response may prove unworkable in a control in this speed region. The partial-stall amplitude again became pronounced as critical pressure was approached.

The attenuation in the compressor-discharge total-pressure response is low at 75.0 percent rated speed (fig. 16(e)). However, during surge, critical pressure was reached at the peak of every cycle. But the peak pressure did not correspond to the peak fuel flow. Once the compressor had started to surge, it did so at a frequency different from that of the oscillatory fuel flow and at an amplitude independent of fuel flow. It required a fuel flow change greater than the superimposed variation to recover from surge.

According to these results, optimizing by the proposed technique is difficult for this turbojet engine. However, for these results the oscillating fuel flow was not held near the critical point but was allowed to continue to increase into the stall region. Also, the data were not completely analyzed. If the critical point in fuel flow were maintained during the acceleration by a complete optimizing control, stall and surge may have been avoided. There appears some hope of an optimizing control working.

Probing into the stall zone by fuel manipulation in an effort to establish maximum compressor-discharge total pressure (or maximum acceleration) is difficult. The difficulties for this type of control are the abrupt pressure drop at stall and the associated hysteresis connected with stall recovery. In addition, combustion lag further complicates the design of such a control.

Examination of Engine Damage

It was desired to determine whether extensive damage was done to the engine during the described engine testing. Several hundred accelerations, each lasting less than 5 seconds, were performed over a period of 65 hours of engine operation. Many of the accelerations experienced not only stall but screech, surge, and blow-out. The only damage found at engine overhaul was loose stator blades in the first and second stator stages of the compressor. The degree of looseness was sufficient to make replacement necessary.

The turbine diaphragm, rotor blades, and so forth, exhibited no cracks, excessive oxidation, or creep. The fuel control system specifically designed for this test allowed excursions into the surge and stall regions and return to steady-state conditions before the turbine

blades, and so forth, had time to reach rated temperatures. It is believed that the fuel system permitted this long engine life under the severe conditions. Surging was sufficiently violent to collapse a 6-foot length of aluminum inlet ducting between the bellmouth and the compressor inlet.

SUMMARY OF RESULTS

An axial-flow turbojet engine was operated on a sea-level static test stand for engine acceleration studies. By using an improved system of instrumentation and a specially designed fuel control system, an investigation of surge and stall behavior for knowledge usable in the design of acceleration control systems yielded the following information:

The engine operated in a partially stalled condition throughout most of the steady-state speed range. This condition resulted in the formation of two or more regions of partial stall propagating at a fraction of engine speed. Partial stall produced no abrupt change in effective discharge pressures or acceleration during fuel flow manipulation.

Accelerations resulting from large increases in fuel flow caused a transition from a multiregion pattern of partial stall to a single region of stall. Between engine speeds of 40 and 80 percent rated, this single stall region, composed of retarded or perhaps reversed flow, extended axially throughout the compressor and propagated at the same fraction of engine speed as did partial stall. This stall behavior was characterized by discontinuities in effective compressor-discharge pressure and abrupt changes in acceleration. Above a speed of 53.0 percent rated, stall was usually preceded by a part, or number, of surge cycles.

A single stall region extended axially throughout the compressor with very little twist. Neglecting this, all compressor stages appeared to stall simultaneously. However, pressure fluctuations due to stall did not appear in the tail cone, being apparently filtered by the combustion process. The frequency and the amplitude of stall appeared independent of fuel flow beyond that required for stall. Both the frequency and the amplitude, however, are related to engine speed. In the midspeed range the limiting value of compressor pressure ratio appeared to be single valued and continuous when determined for both surge and stall.

Surge appeared possible only when the compressor-discharge total-pressure drop at stall exceeded 16 percent. As contrasted with stall, its frequency was dependent upon both speed and fuel flow, and perhaps on the large volumes associated with combustors and tail cones. The compressor-discharge total pressure reached critical pressure during each cycle of surge.

Surge accompanied by stall occurred only at critical pressure, which was always the maximum pressure reached; maximum acceleration was always coincident with critical pressure. Surge and stall initiation also appeared insensitive to the rate of increase in fuel flow.

Combustion delay was present. It was of approximately 30-millisecond duration and appeared to consist of the following times: transport time between throttle and nozzles, dead time in the combustors (mixing and transport), and lag in the combustors (burning process). Post-turbine, or tail-pipe, burning due to localized enriched mixtures during stall appeared to add to hysteresis time. This time, the time required for the compressor to recover from stall, depended on the amount of fuel burning in the tail pipe, and it ranged from some arbitrarily long time (due to blow-out) to practically zero time. This minimum time resulted only from momentary stall approaches with limiting fuel flows.

The only stall warning observed appeared in a very limited speed range (65.4 to 73.0 percent rated). It consisted of a momentary magnification of the partial-stall pattern immediately preceding stall.

Application of optimizing types of acceleration control appears difficult for this engine because of the discontinuities in pressures at stall, hysteresis effects resulting from stall, and combustion lag.

Lewis Flight Propulsion Laboratory
National Advisory Committee for Aeronautics
Cleveland, Ohio, September 16, 1954

3484

APPENDIX A

SYMBOLS

The following symbols are used in this report:

N	engine speed, percent rated rpm
P	pressure, lb/sq in.
V	velocity, ft/sec
W	fuel flow, lb/hr
δ	ratio of pressure to NACA standard sea-level pressure
θ	ratio of temperature to NACA standard sea-level temperature
λ	fuel-valve position, in.
ρ	density, lb/cu ft
ρV	specific weight flow, lb/(sec)(sq ft)
σ	stress, psi
ϕ	phase angle, deg
ω	frequency, cps

Subscripts:

f	fuel
l	large slot
s	small slot
t	throttle discharge
0	compressor inlet
1,2,3...	compressor stages
12	compressor discharge
13	turbine discharge

APPENDIX B

INSTRUMENTATION

Consideration of engine life had dictated, for these tests, new data-taking techniques and modified engine operational procedures. In order to make these possible, instrumentation possessing good frequency response and maintaining accurate calibration during dynamic behavior was required. The frequency-response range needed was determined by performing a survey of air flow fluctuations with constant-temperature hot-wire anemometers. Useful information appeared below a frequency of 150 cycles per second; only the fundamental and first harmonic of the blade wake appeared above the "noise" level in the region above 150 cycles per second.

Air flow measurements based on sensing dynamic pressures at any single point could not yield the instantaneous average flow, especially during stalled or surged engine conditions. The anemometers used not only were short-lived in engine testing but were incapable of sensing the direction of flow (reverse flow was rectified). Temperature measurements at the stall frequencies required compensated thermocouples, but they were not used. Compensation is based on fixed lags in the sensing system; however, mass flow fluctuated during stall and surge, and at times also reversed, causing the thermocouple time constant to vary accordingly. As a result, the output of the compensated thermocouples contained large errors during varying air flows. Because of the above limitations, total-pressure probes were used that were designed to pass up to 150 cycles per second. This dependence on total-pressure measurements was based on recordings such as figure 17, on which it is indicated that total pressures and mass flow variations as measured by hot wires were in phase during stalled engine conditions.

The location of the total-pressure probes is shown in figure 2. All the pressure probes were made as nearly identical as possible. The dynamic characteristics are given in figure 18 for standard sea-level gas conditions. The underdamped response resulted from the desire for a high natural frequency and the mechanical limitations of pressure-probe construction (ref. 9).

Speed measurement was accomplished with an alternator which was directly coupled to the compressor shaft and which produced 180 cycles every engine revolution. The alternator output was demodulated with a frequency meter which supplied a carefully filtered signal to an amplifier containing appropriate zeroing and gain adjustments. The amplifier simultaneously drove a galvanometer element and provided a monitoring signal to an oscilloscope. This combination permitted a continuously visible recording of the speed variation. The alternator also supplied

a signal to a variable time base counter whose display periodically flashed the actual rpm for that period of counting.

Fuel flow measurements were obtained by recording the small-slot fuel pressure at one of the fuel nozzles. The difference between this pressure and the compressor-discharge total pressure was a measure of the flow at any instant.

Stress measurements in each of the 12 stator stages were obtained by instrumenting one blade in each stage with two bonded strain gages placed at that point which produced maximum stresses due to bending and minimum stresses due to twisting. Two additional dummy gages were imbedded in the compressor housing to minimize temperature errors, thus comprising a temperature-compensated balanced bridge.

All air pressures, fuel pressures, and stresses were sensed by balanced strain-gage transducers. The outputs were amplified by conventional carrier amplifiers incorporating balance and gain adjustments which drove appropriate galvanometers in a 16-channel recording oscillograph.

All gradients on the oscillograph traces were obtained by subjecting the individual transducers to known fixed pressures. The stress sensitivities were computed from the known gage factors and blade material, because it wasn't necessary to determine the absolute magnitude of the stresses for this study. Speed sensitivity was obtained at various points of the speed range by introducing a known frequency change into the frequency meter. Fuel flow at any instant was determined by measuring the pressure drop across the nozzles (small-slot fuel pressure minus compressor-discharge total pressure) and referring to figure 19 for the actual fuel flow. The linear relation shown in this figure resulted from the flow-divider design. Because the natural frequency of the flow divider and of the entire fuel system was high (appendix C), the instantaneous pressure drop across the nozzles was considered a measure of the fuel flow at low frequencies.

A steady-state plot of the necessary engine variables was obtained throughout the speed range. At each initial-speed condition, before the acceleration attempt, the preceding steady-state values were assumed. Thus, the known recording sensitivities, together with the initial steady-state values, were sufficient to calibrate each recording.

APPENDIX C

FUEL SYSTEM

The technique of probing the stall and surge region of a turbojet engine with short pulses of fuel flow required a fuel control system that responded very rapidly to changes of the control setting. Therefore, the existing throttle (sleeve-piston type) was isolated from the engine system and was driven by an electrohydraulic servomotor possessing an essentially flat response to 100 cycles per second. The fuel source was an independent 14,000-pound-per-hour pump, and all the "flex hose" containing high pressures between the pump and the flow divider was replaced with 1-inch copper tubing.

In order to obtain the lowest-impedance fuel supply to the pump, fuel was made to flow into an automatic-level-controlled header tank. Supply at gravity pressure to the pump inlet was then achieved with a 2-inch-pipe connection to the header tank and $2\frac{1}{2}$ -gallon accumulator at the pump inlet (fig. 20). A pressure-regulating relief valve, based on the design considerations presented in reference 10, was installed, and it maintained a constant pressure drop of 100 pounds per square inch across the throttle. Its natural frequency of 170 cycles per second (fig. 8(b)) and the natural frequency of 80 cycles per second for the flow divider (fig. 8(c)) permitted the "stiff" fuel system to resonate at a high enough frequency (33 cps from fig. 8(b)) to allow an increase in fuel flow to 8000 pounds per hour in approximately 0.010 second.

The fuel system (fig. 20) was capable of following electric signals from high-impedance sources such as computers, signal generators, and so forth. Its response to an audio oscillator (fig. 6) indicated flow responses to high frequencies. The fuel-system resonance at 33 cycles per second checked with the "ringing" in small-slot pressure shown in figure 8(b). Transport time (time difference between a pressure change at the pump discharge and corresponding pressure change at the fuel nozzle) was of the order of 0.010 second (fig. 8(a)).

REFERENCES

1. Lucas, James G., and Filippi, Richard E.: Multiple Over-All Performance and Rotating Stall Characteristics of a 15-Stage Experimental Axial Flow Compressor at an Intermediate Speed. NACA RM E54C29, 1954.
2. Donlon, Richard H., McCafferty, Richard J., and Straight, David M.: Investigation of Transient Combustion Characteristics in a Single Tubular Combustor. NACA RM E53L10, 1954.

3. Stiglic, Paul M., Schmidt, Ross D., and Delio, Gene J.: Experimental Investigation of Acceleration Characteristics of a Turbojet Engine Including Regions of Surge and Stall for Control Applications. NACA RM E54H24, 1955.
4. Oppenheimer, Frank L., and Pack, George J.: Investigation of Acceleration Characteristics of a Single-Spool Turbojet Engine. NACA RM E53H26, 1953.
5. Iura, T., and Rennie, W. D.: Experimental Investigations of Propagating Stall in Axial-Flow Compressors. Trans. A.S.M.E., vol. 76, no. 3, Apr. 1954, pp. 463-471.
6. Huppert, Merle C., and Benser, William A.: Some Stall and Surge Phenomena in Axial-Flow Compressors. Jour. Aero. Sci., vol. 20, no. 12, Dec. 1953, pp. 835-845.
7. Huppert, Merle C., Costilow, Eleanor L., and Budinger, Ray E.: Investigation of a 10-Stage Subsonic Axial-Flow Research Compressor. III - Investigation of Rotating Stall, Blade Vibration, and Surge at Low and Intermediate Compressor Speeds. NACA RM E53C19, 1953.
8. Draper, C. S., and Li, Y. T.: Principles of Optimizing Control Systems and Application to the Internal Combustion Engine. Aero. Eng. Dept., M.I.T., pub. by A.S.M.E., Sept. 1951.
9. Delio, Gene J., Schwent, Glennon V., and Cesaro, Richard S.: Transient Behavior of Lumped-Constant Systems for Sensing Gas Pressure. NACA TN 1988, 1949.
10. Gold, Harold, and Otto, Edward W.: An Analytical and Experimental Study of the Transient Response of a Pressure-Regulating Relief Valve in a Hydraulic Circuit. NACA TN 3102, 1954.

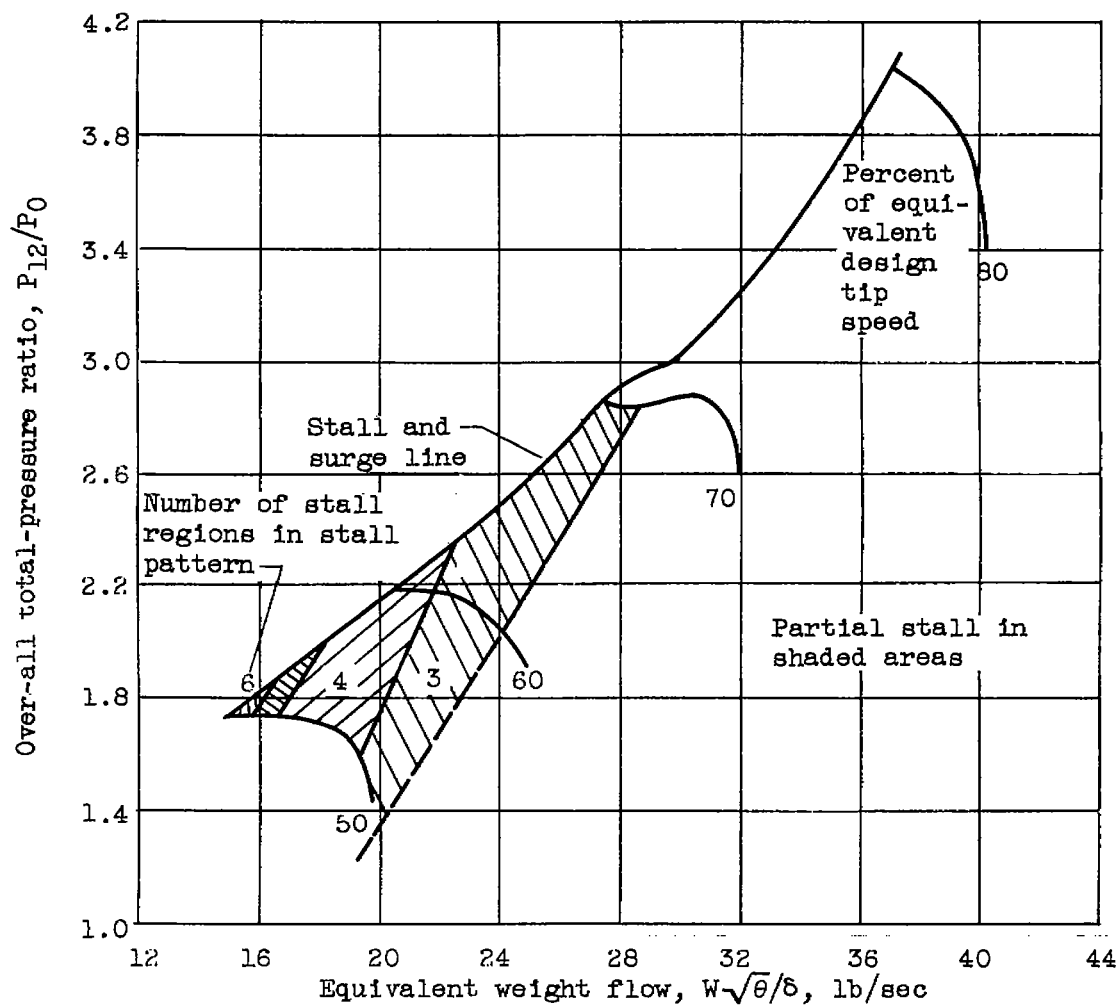


Figure 1. - Over-all compressor performance map of a typical compressor.

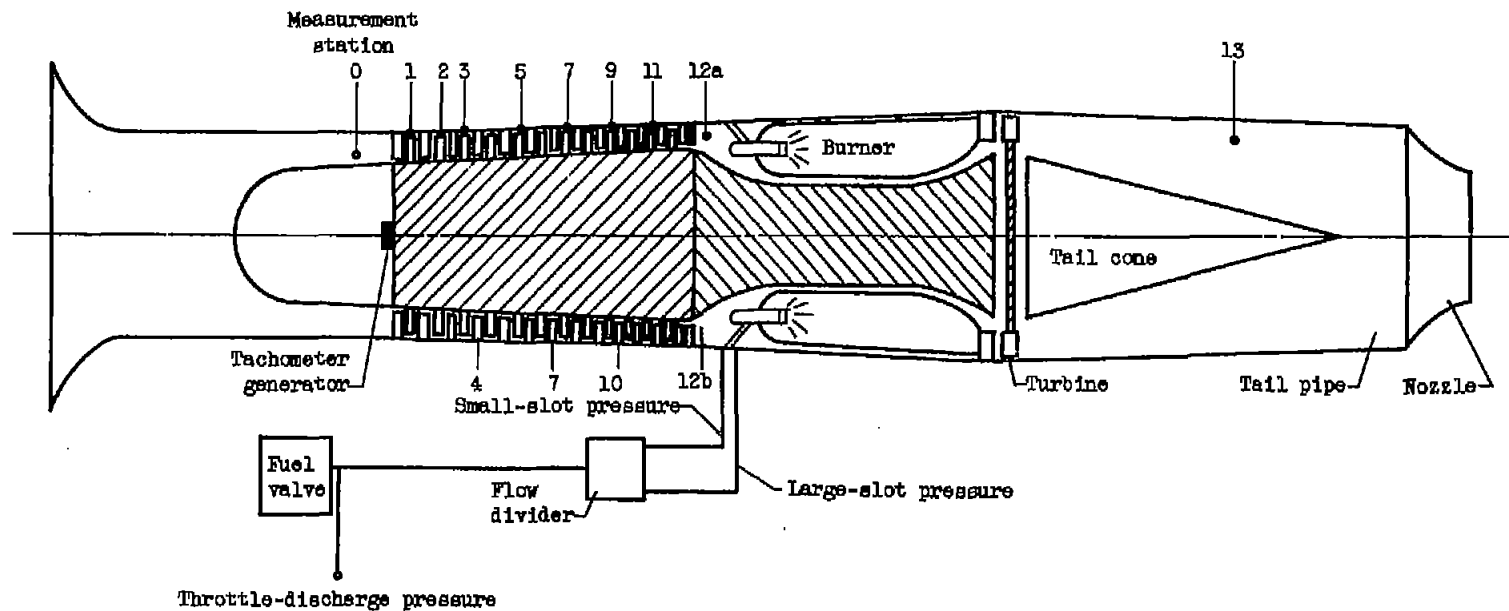
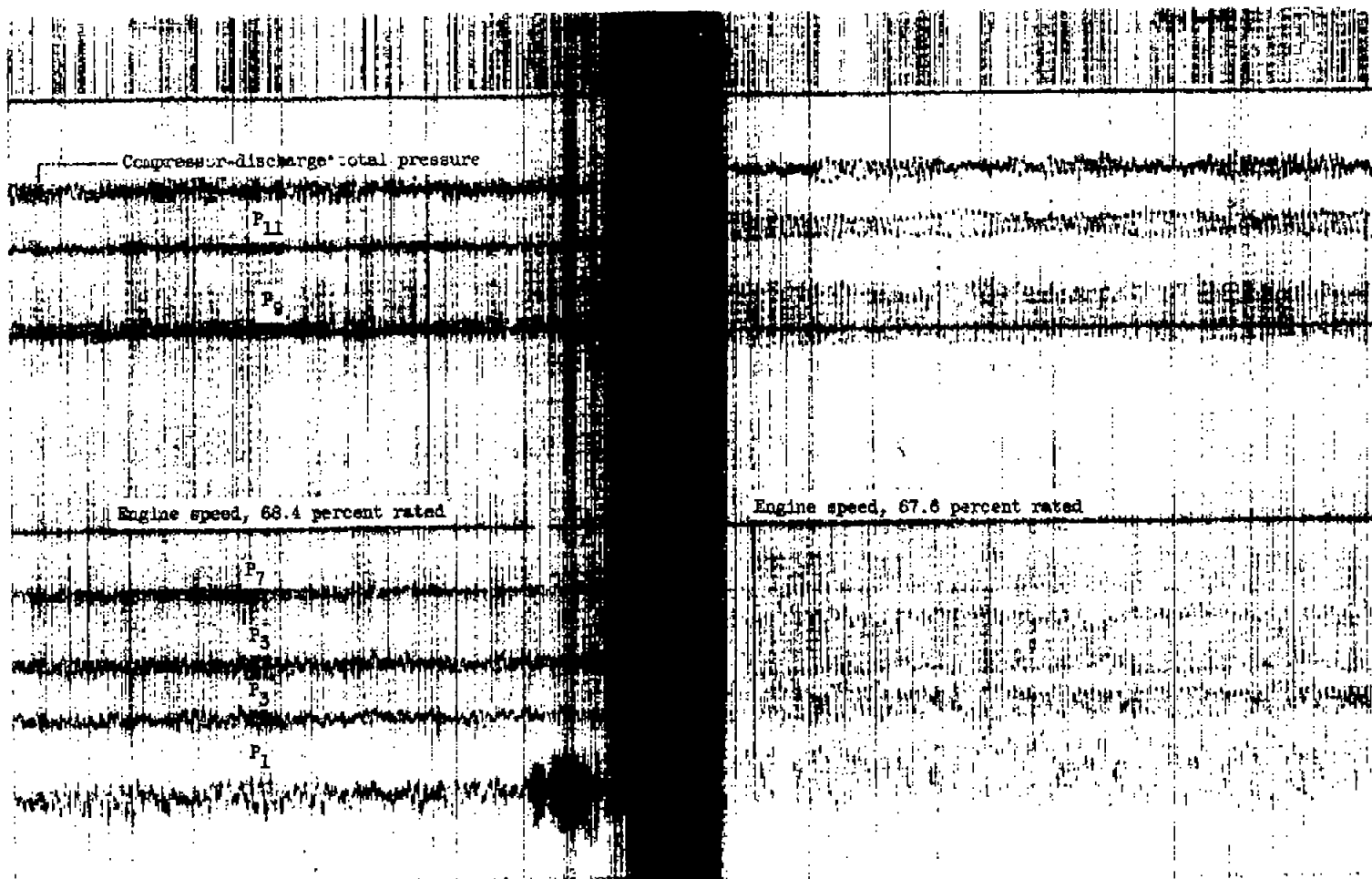
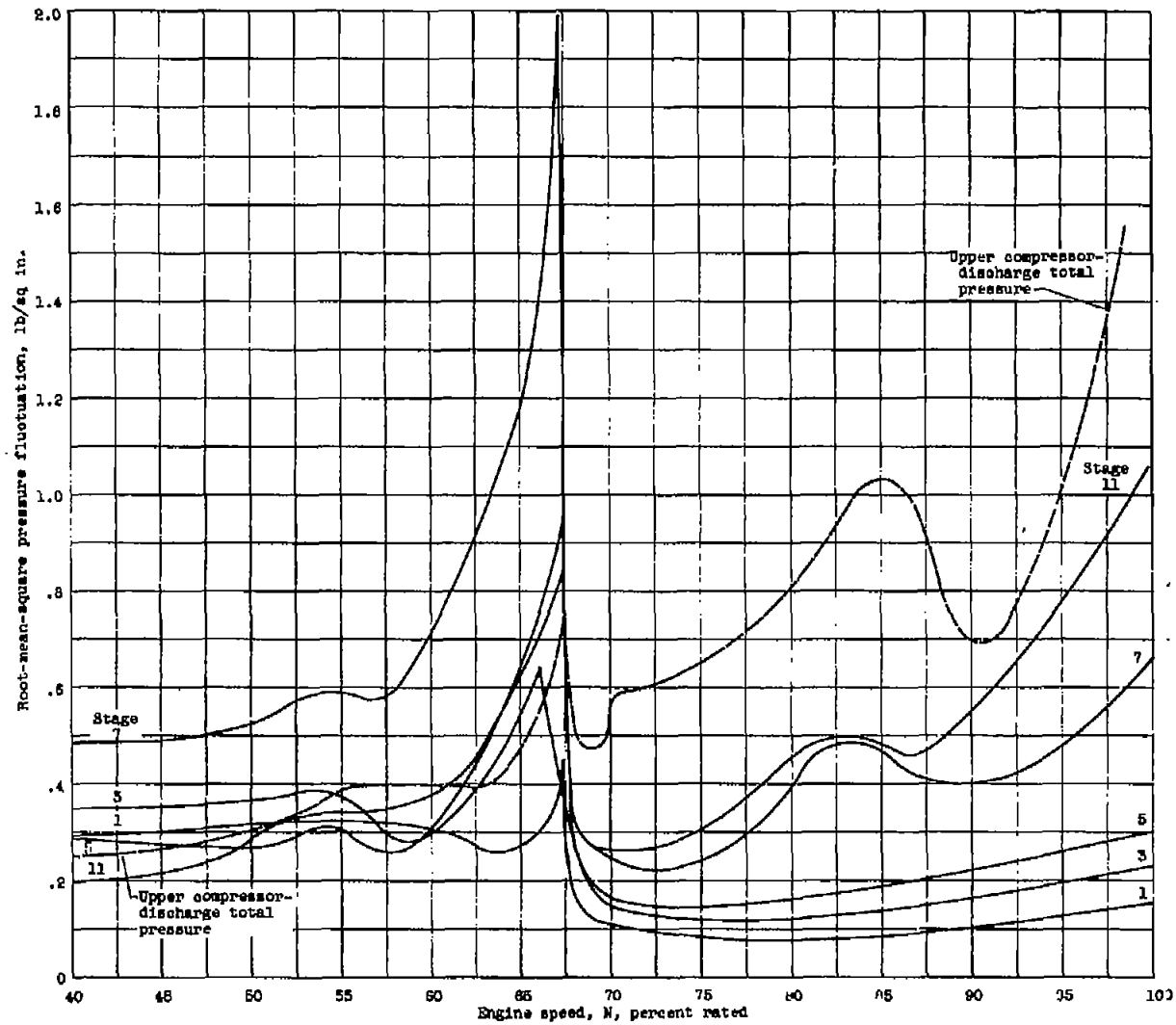


Figure 2. - Schematic representation of turbojet engine and location of measurement stations.



(a) Sample trace.

Figure 3. - Magnitude of pressure fluctuations P existing in compressor during steady-state operation.



(b) Survey throughout speed range.

Figure 3. - Concluded. Magnitude of pressure fluctuations P existing in compressor during steady-state operation.

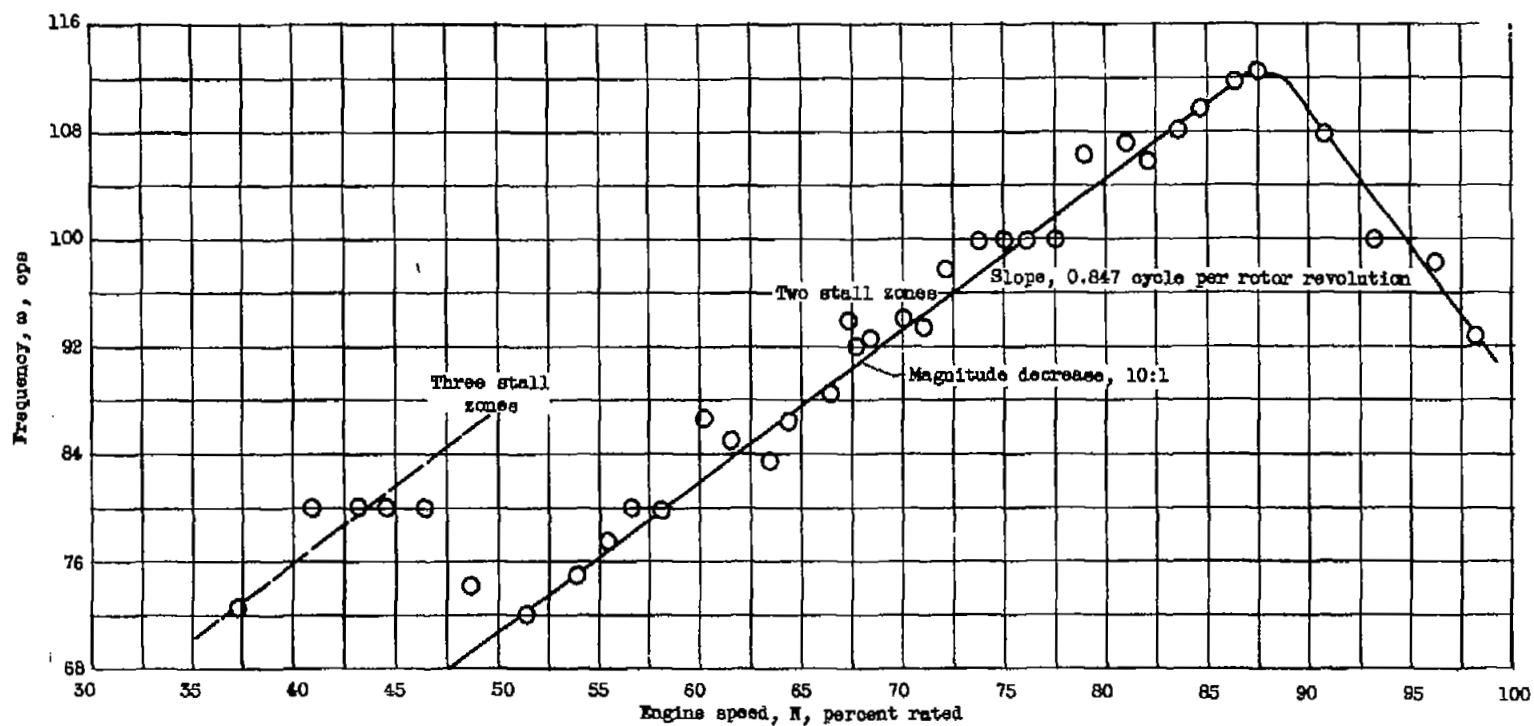
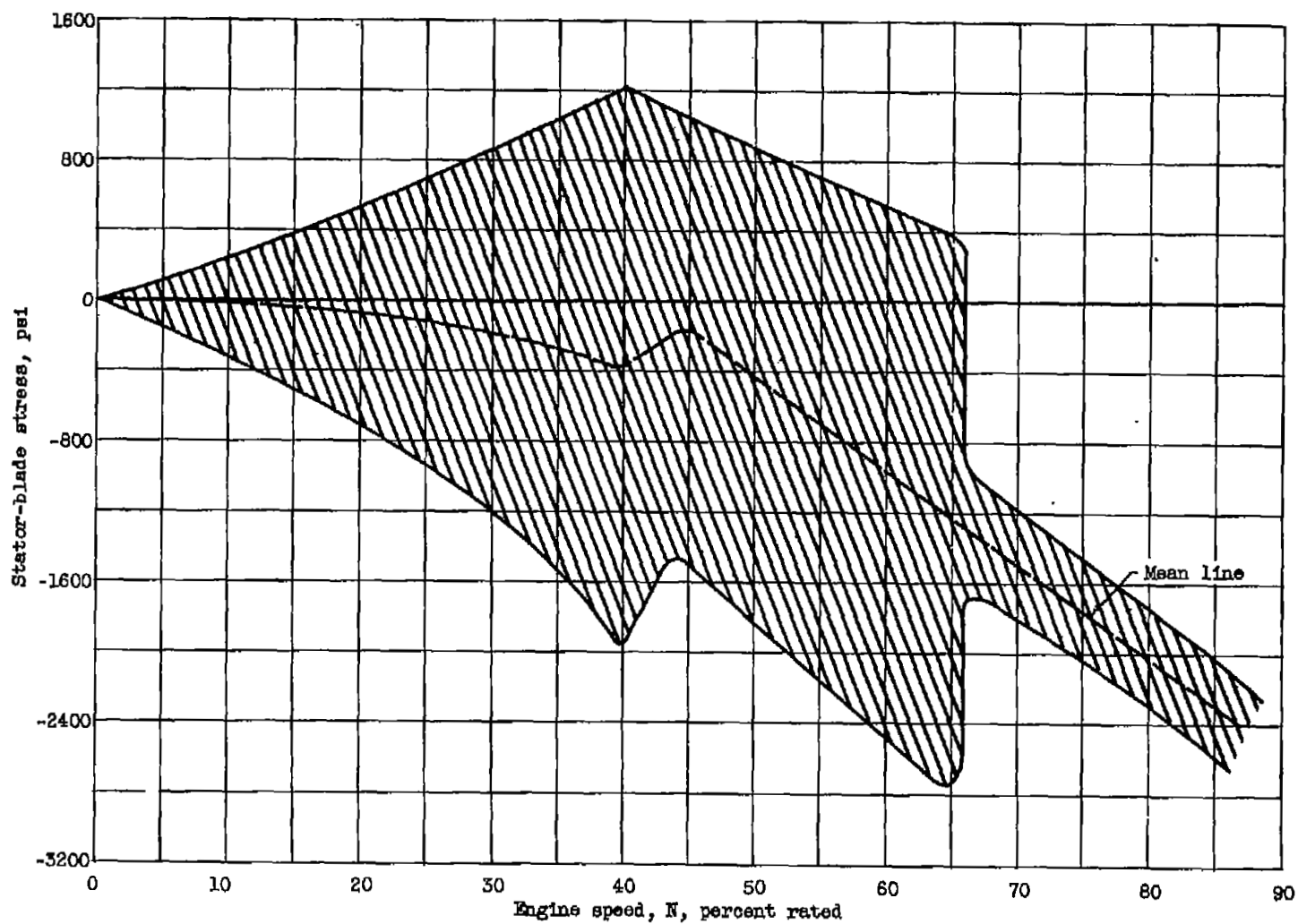
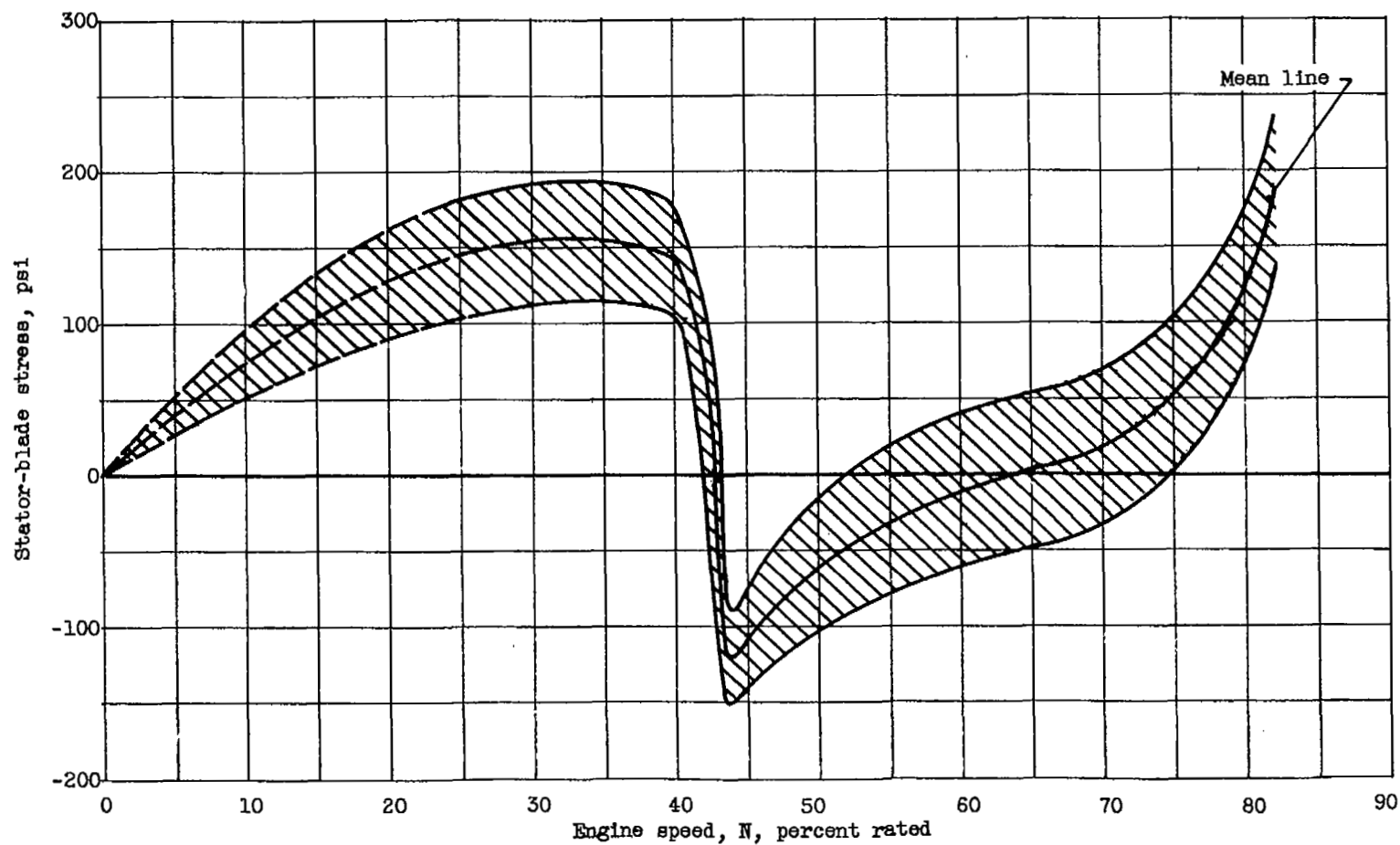


Figure 4. - Frequency of pressure fluctuations existing at compressor discharge during steady-state operation.



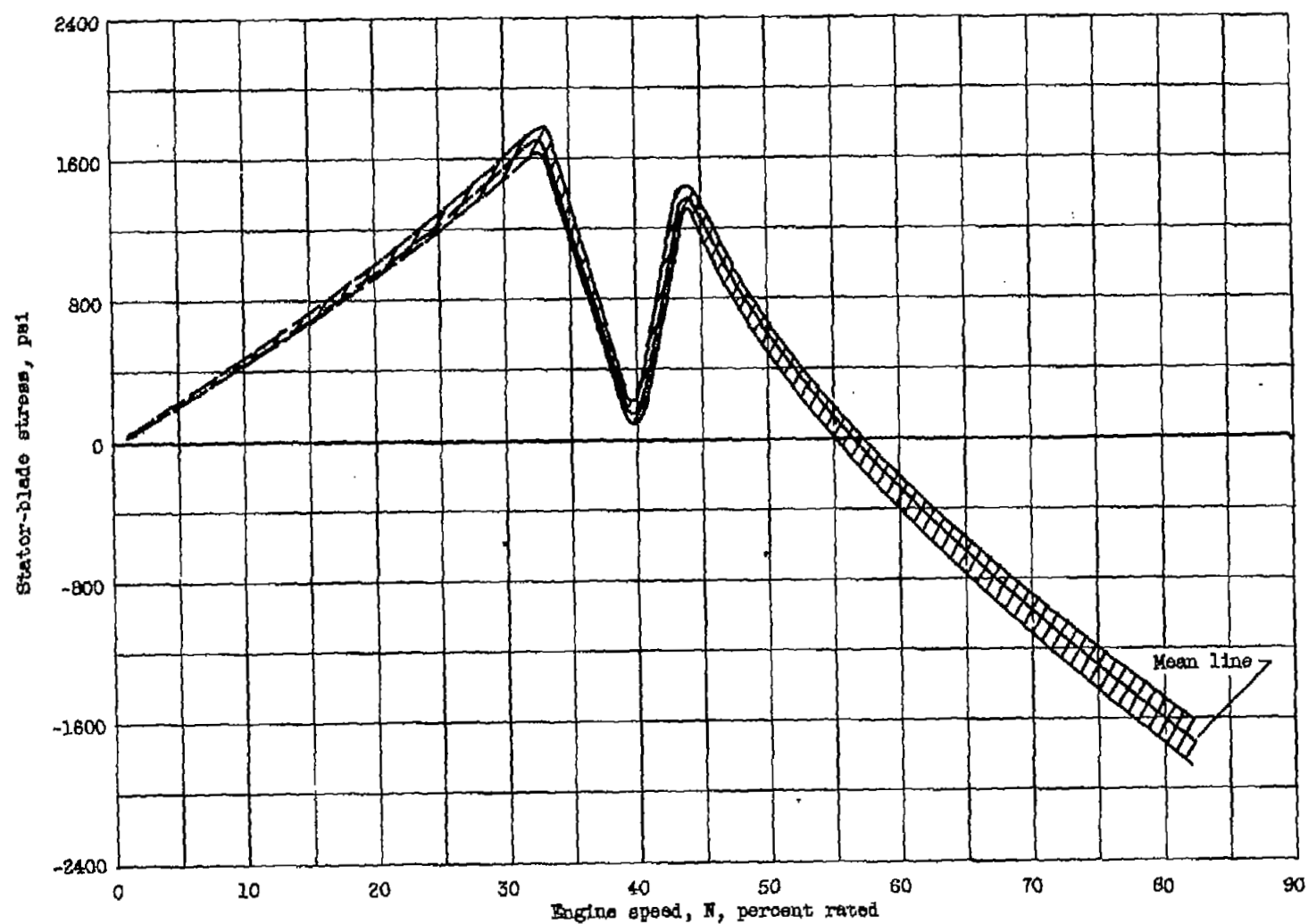
(a) Compressor stage, 4th. Frequency, 330 cycles per second.

Figure 5. - Bending stresses generated in compressor stator blades during steady-state operation.



(b) Compressor stage; 7th. Frequency, 650 cycles per second.

Figure 5. - Continued. Bending stresses generated in compressor stator blades during steady-state operation.



(a) Compressor stage, 10th. Frequency, 940 cycles per second.

Figure 5. - *Continued*. Bending stresses generated in compressor stator blades during steady-state operation.

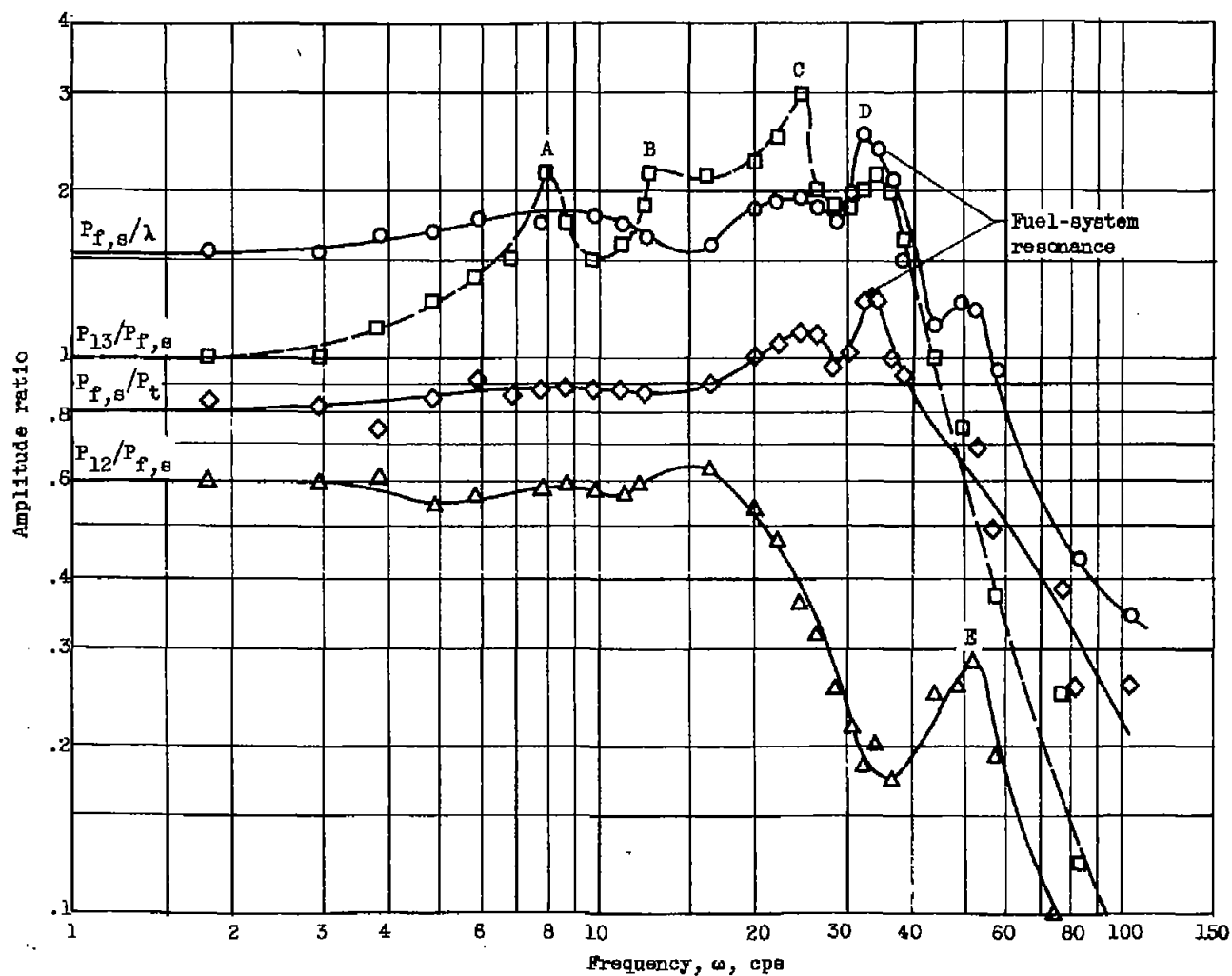


Figure 6. - Response of compressor- and turbine-discharge total pressures to sinusoidal variations of fuel flow. Engine speed, 69.2 percent rated; $P_{f,s}$, small-slot fuel pressure; λ , throttle position; P_{13} , turbine-discharge total pressure; $P_{f,t}$, throttle-discharge fuel pressure; P_{12} , compressor-discharge total pressure.

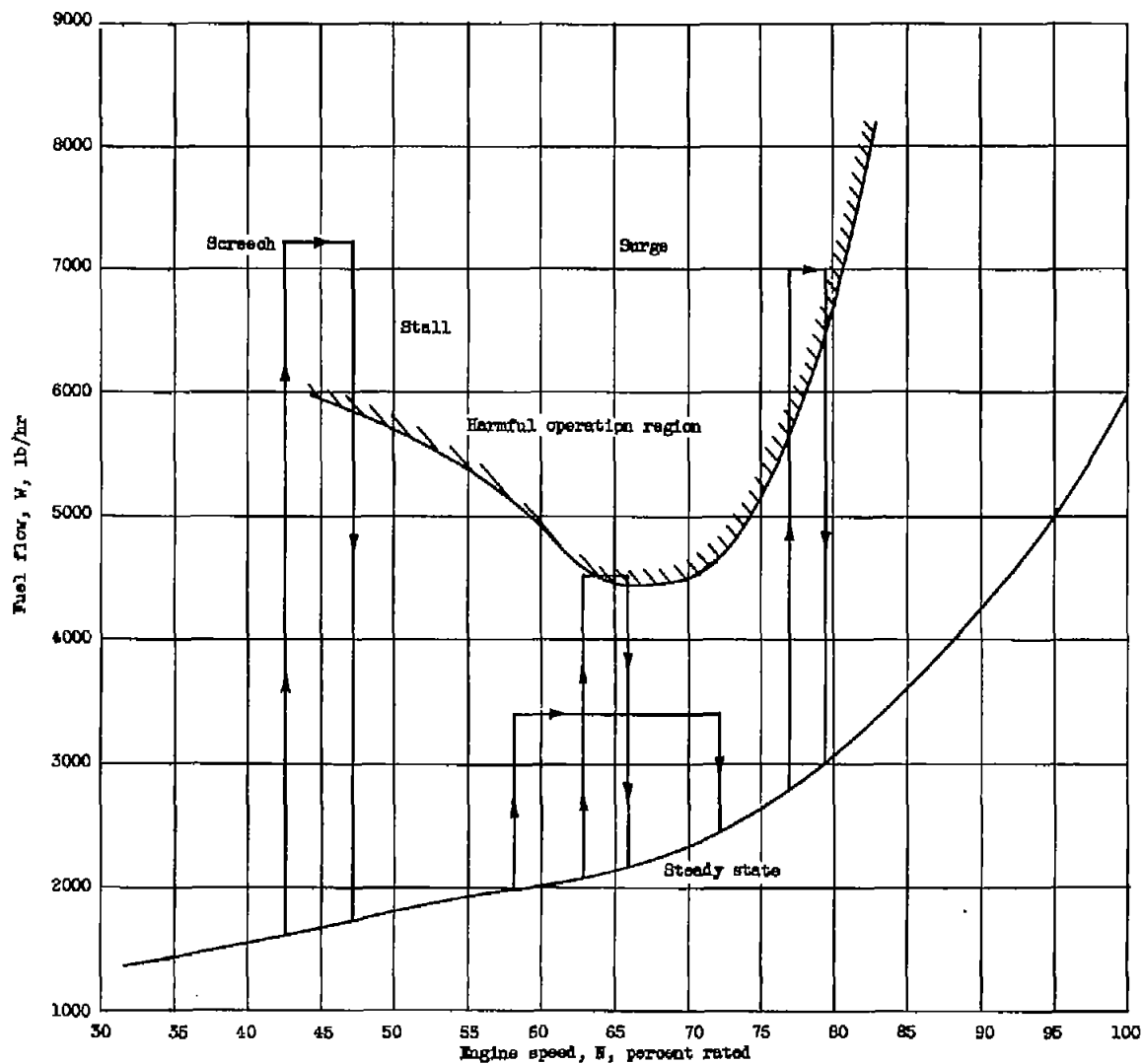
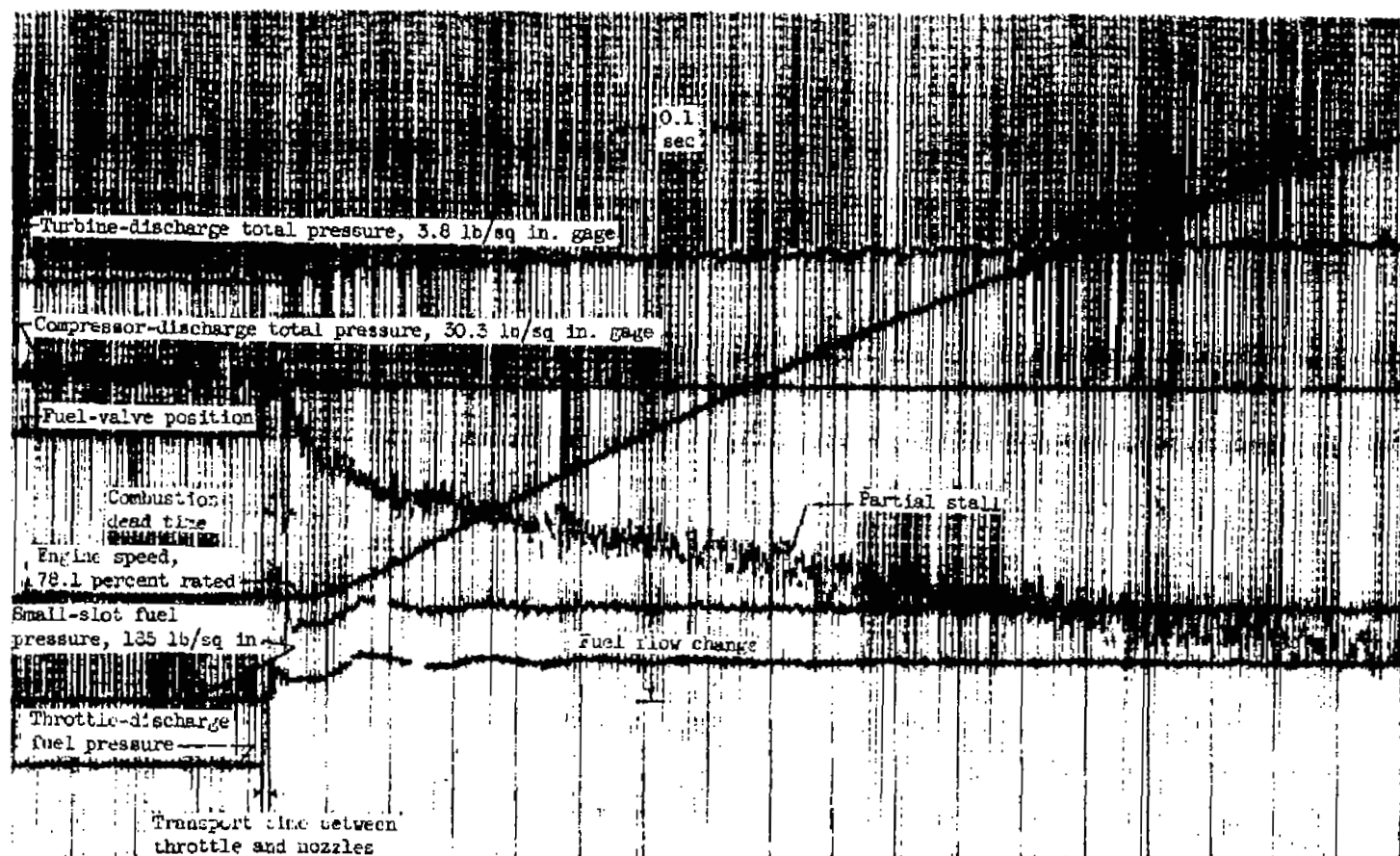
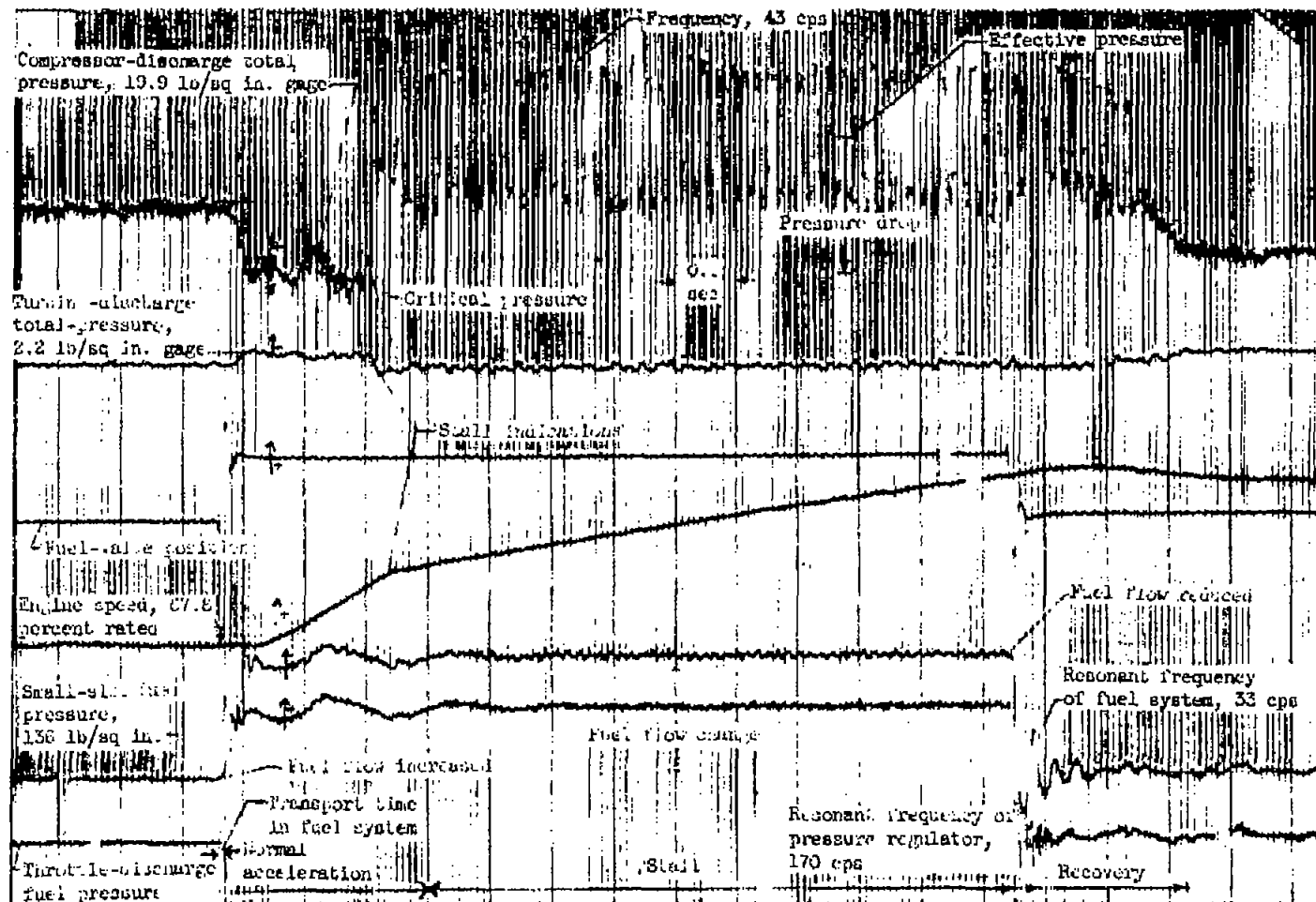


Figure 7. - Fuel flow manipulation during surge and stall studies. Maximum surge-free and stall-free fuel flow for turbojet engine.



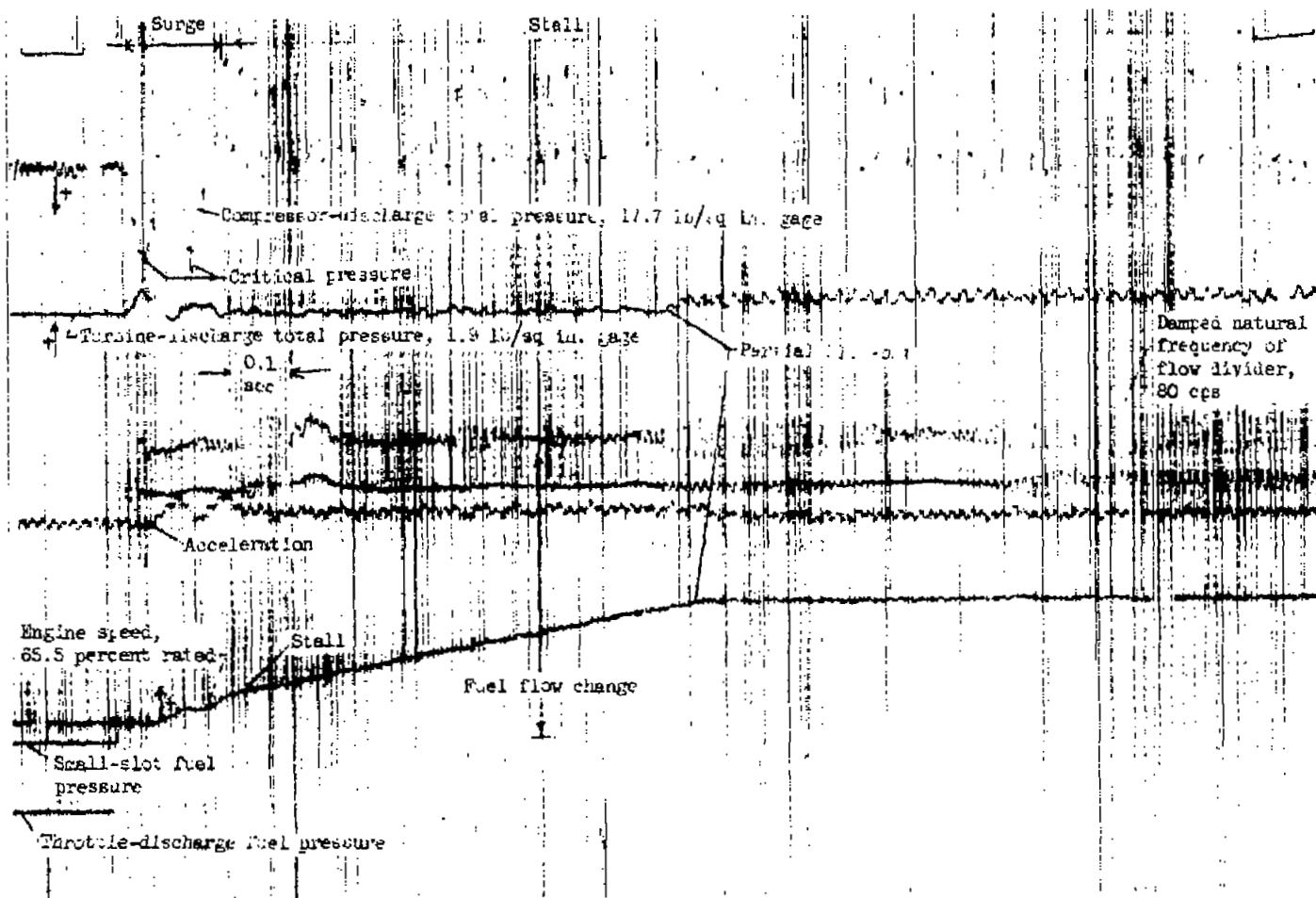
(a) Successful acceleration. Calibration: turbine-discharge total pressure, 8.3((lb/sq in.)/in.); compressor-discharge total pressure, 6.96((lb/sq in.)/in.); engine speed, 2.5 percent rated/(in.); small-slot fuel pressure, 170((lb/sq in.)/in.).

Figure 8. - Effect of step change in fuel flow on engine variables during acceleration.



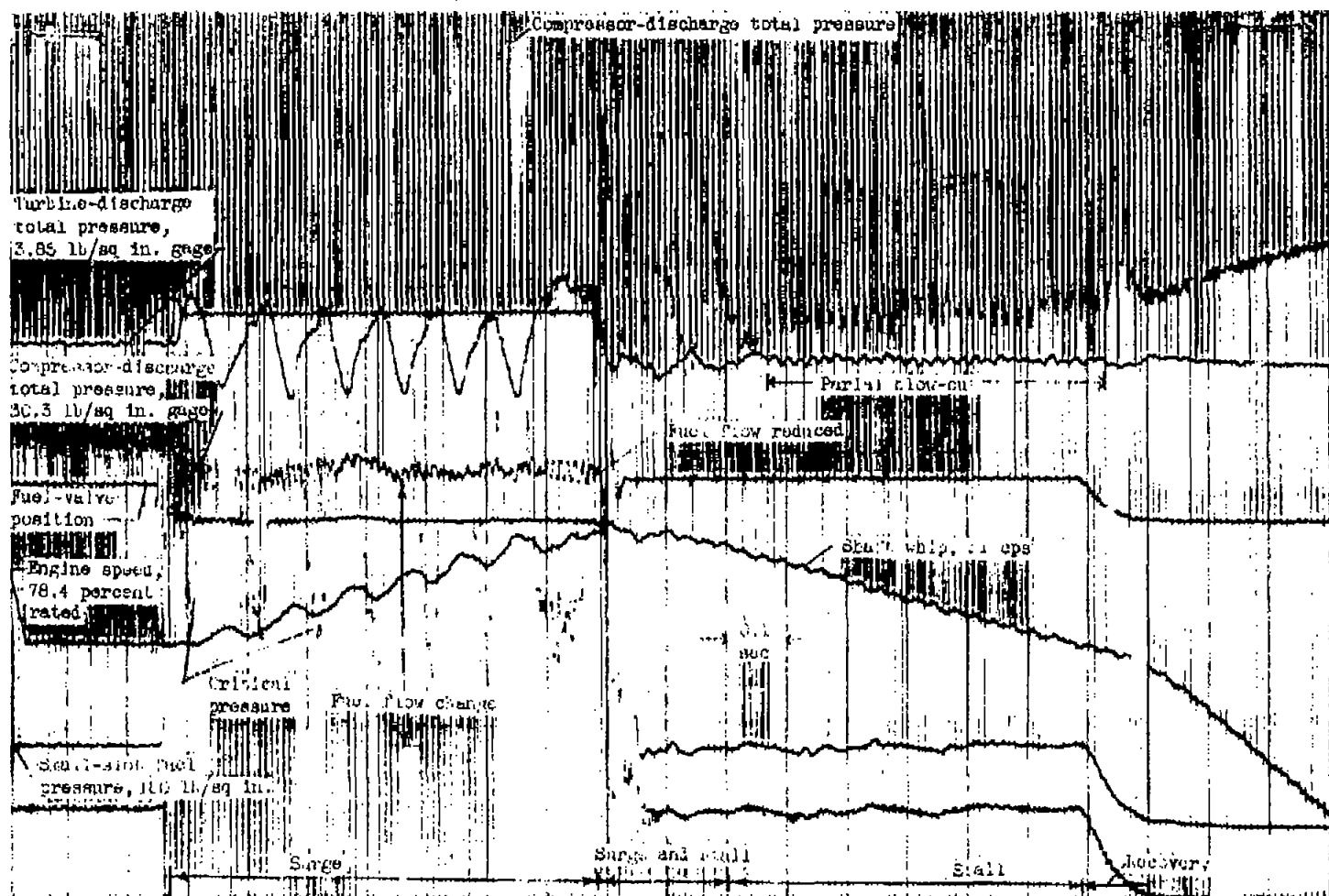
(b) Stall. Calibration: compressor-discharge total pressure, 6.96((lb/sq in.)/in.); turbine-discharge total pressure, 8.5((lb/sq in.)/in.); engine speed, 2.5 percent rated/(in.); small-slot fuel pressure, 171((lb/sq in.)/in.).

Figure 8. - Continued. Effect of step change in fuel flow on engine variables during acceleration.



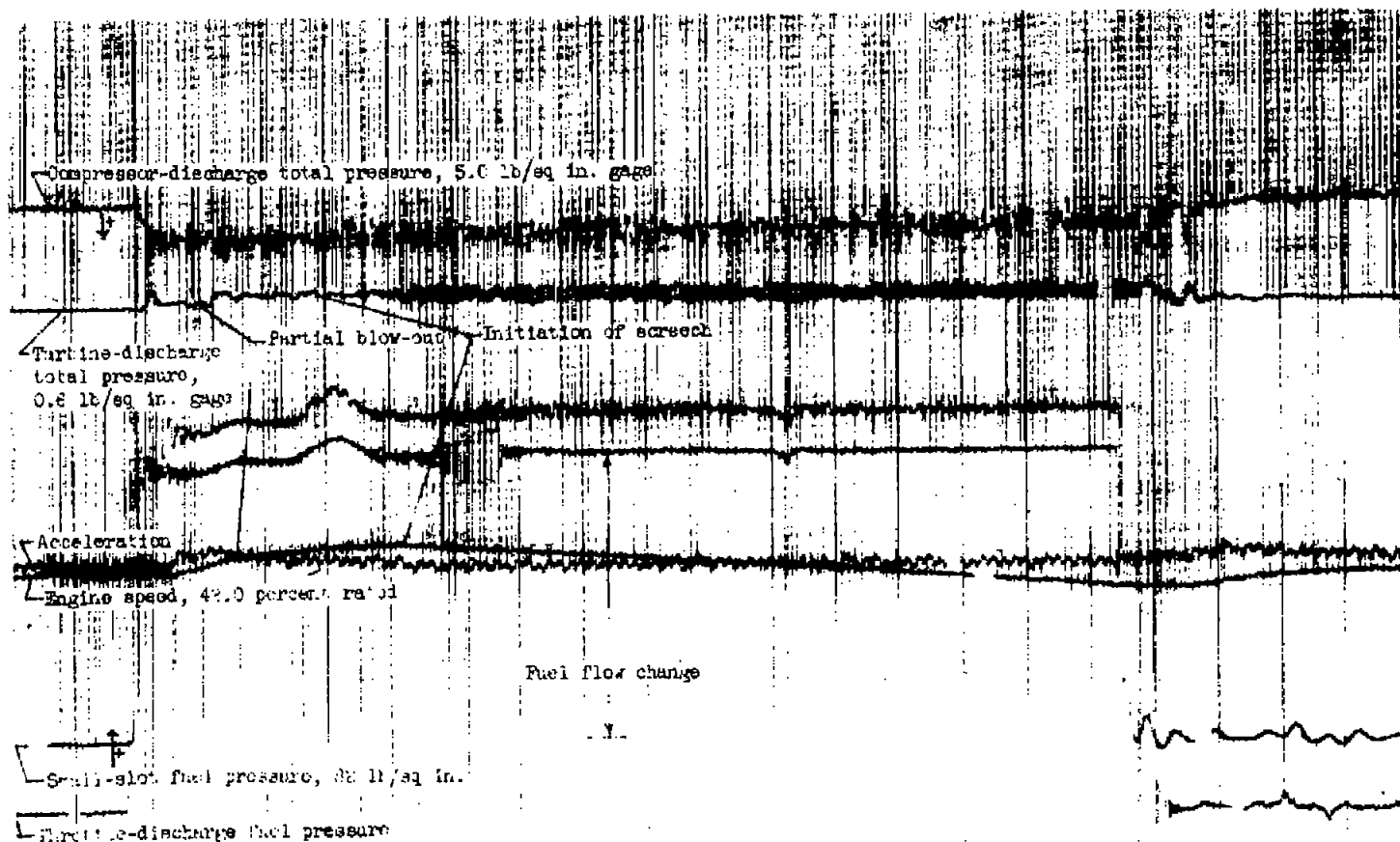
(c) Partial blow-out. Calibration: compressor-discharge total pressure, $6.96((\text{lb/sq in.})/\text{in.})$; turbine-discharge total pressure, $8.18((\text{lb/sq in.})/\text{in.})$; engine speed, 2.5 percent rated/ (in.) ; small-slot fuel pressure, $171((\text{lb/sq in.})/\text{in.})$.

Figure 8. - Continued. Effect of step change in fuel flow on engine variables during acceleration.



(d) Surge. Calibration: turbine-discharge total pressure, 8.3((lb/sq in.)/in.); compressor-discharge total pressure, 6.96((lb/sq in.)/in.); engine speed, 2.5 percent rated/(in.); small-slot fuel pressure, 171((lb/sq in.)/in.).

Figure 8. - Continued. Effect of step change in fuel flow on engine variables during acceleration.



(e) Screech. Calibration: compressor-discharge total pressure, 6.96((lb/sq in.)/in.); turbine-discharge total pressure, 8.18((lb/sq in.)/in.); engine speed, 2.5 percent rated/(in.); small-slot fuel pressure, 170((lb/sq in.)/in.).

Figure 8. - Concluded. Effect of step change in fuel flow on engine variables during acceleration.

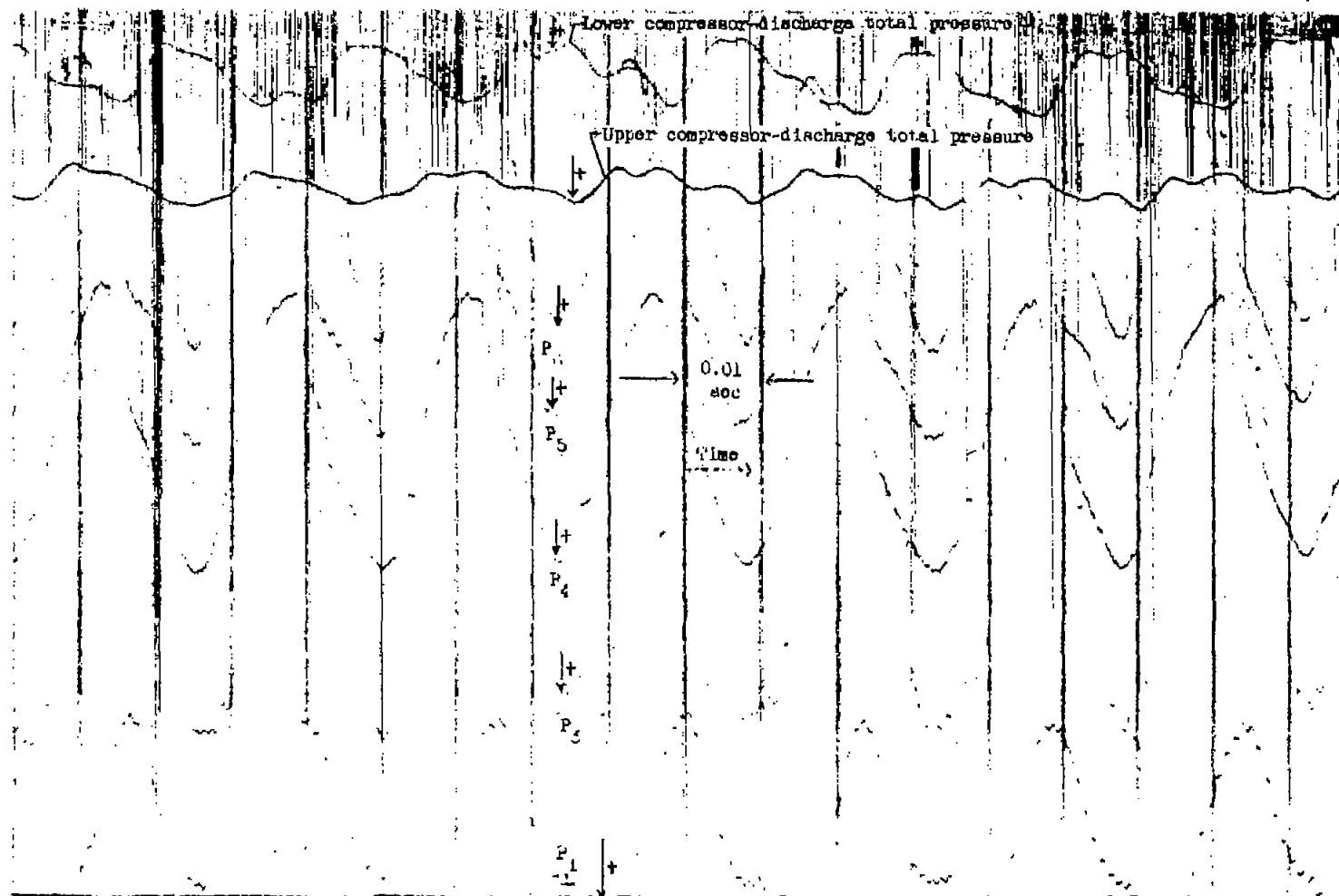


Figure 9. - Phase relation of various stage total pressures P existing in stalled compressor.

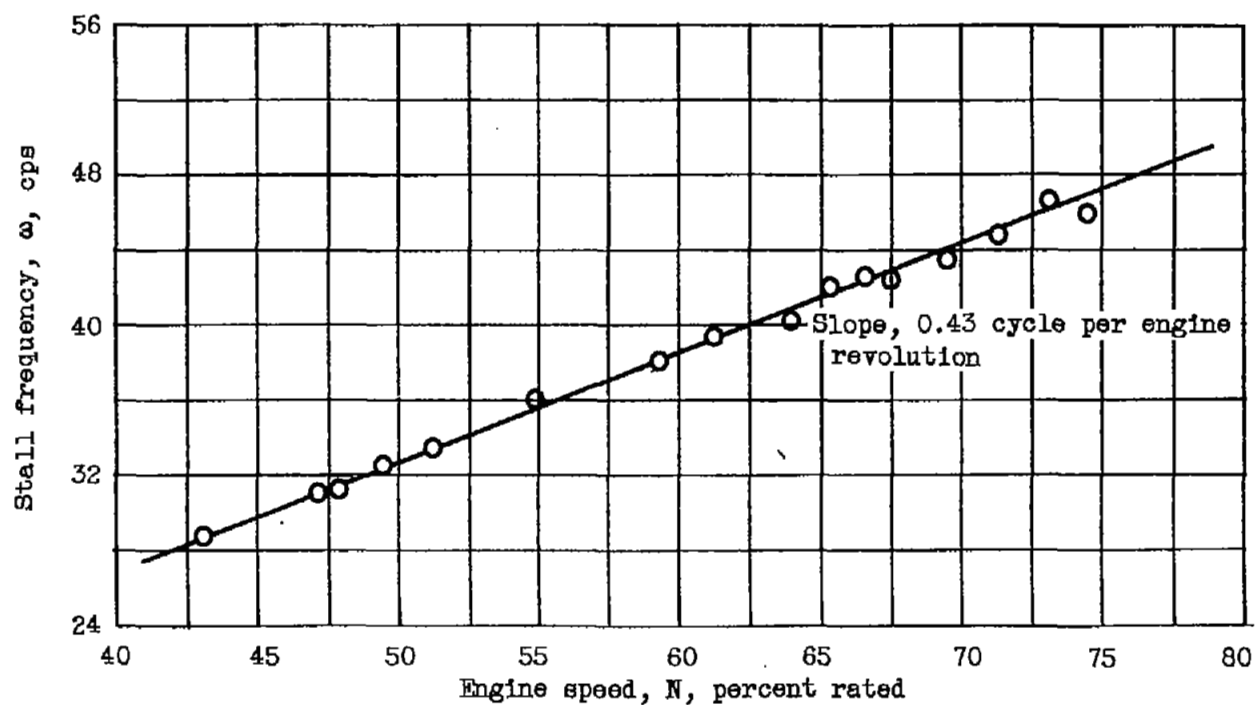
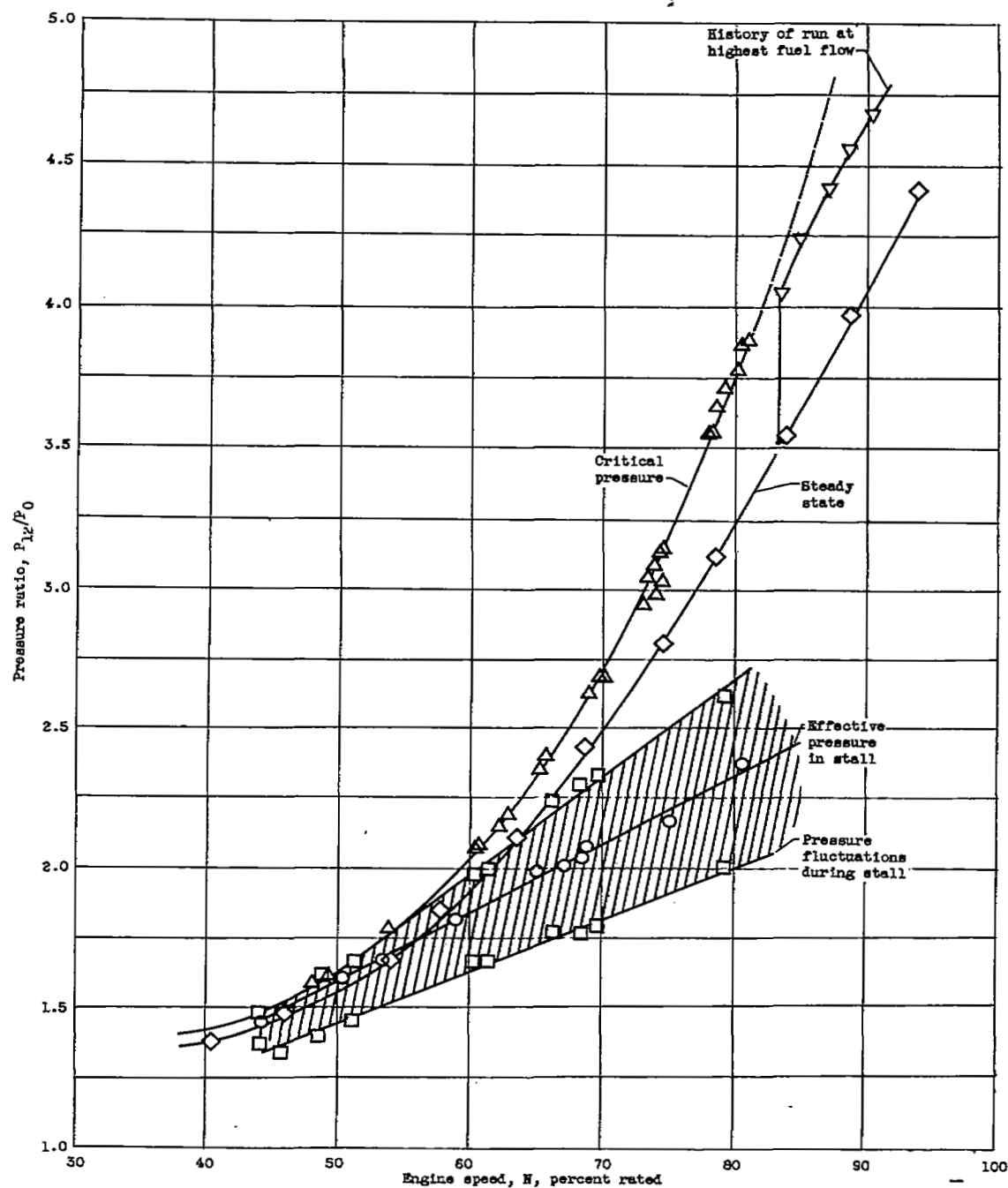
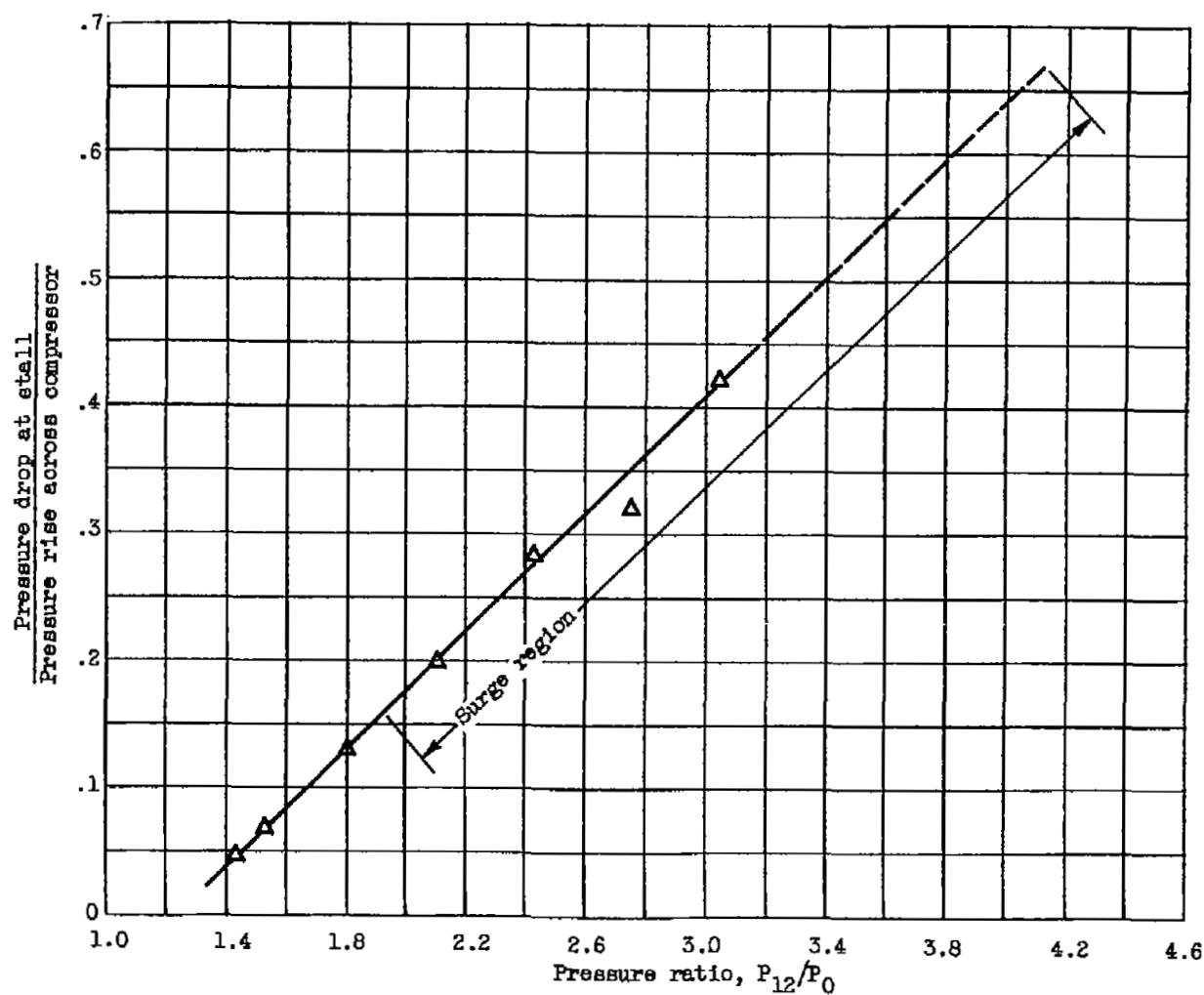


Figure 10. - Propagation rate of stall obtained during acceleration.



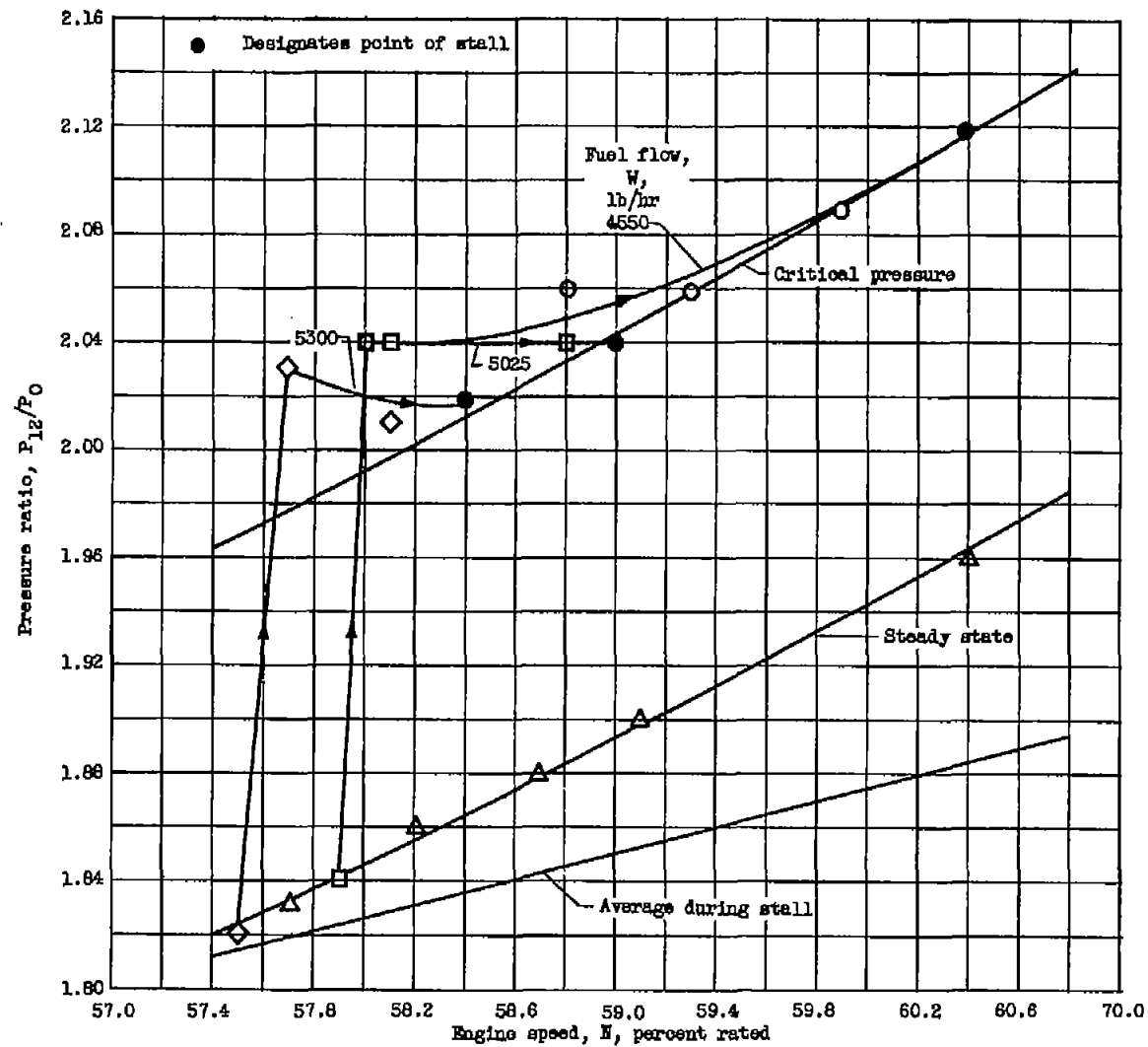
(a) Maximum pressure obtainable and region of pressure fluctuation during stall.

Figure 11. - Pressure ratio developed during acceleration.



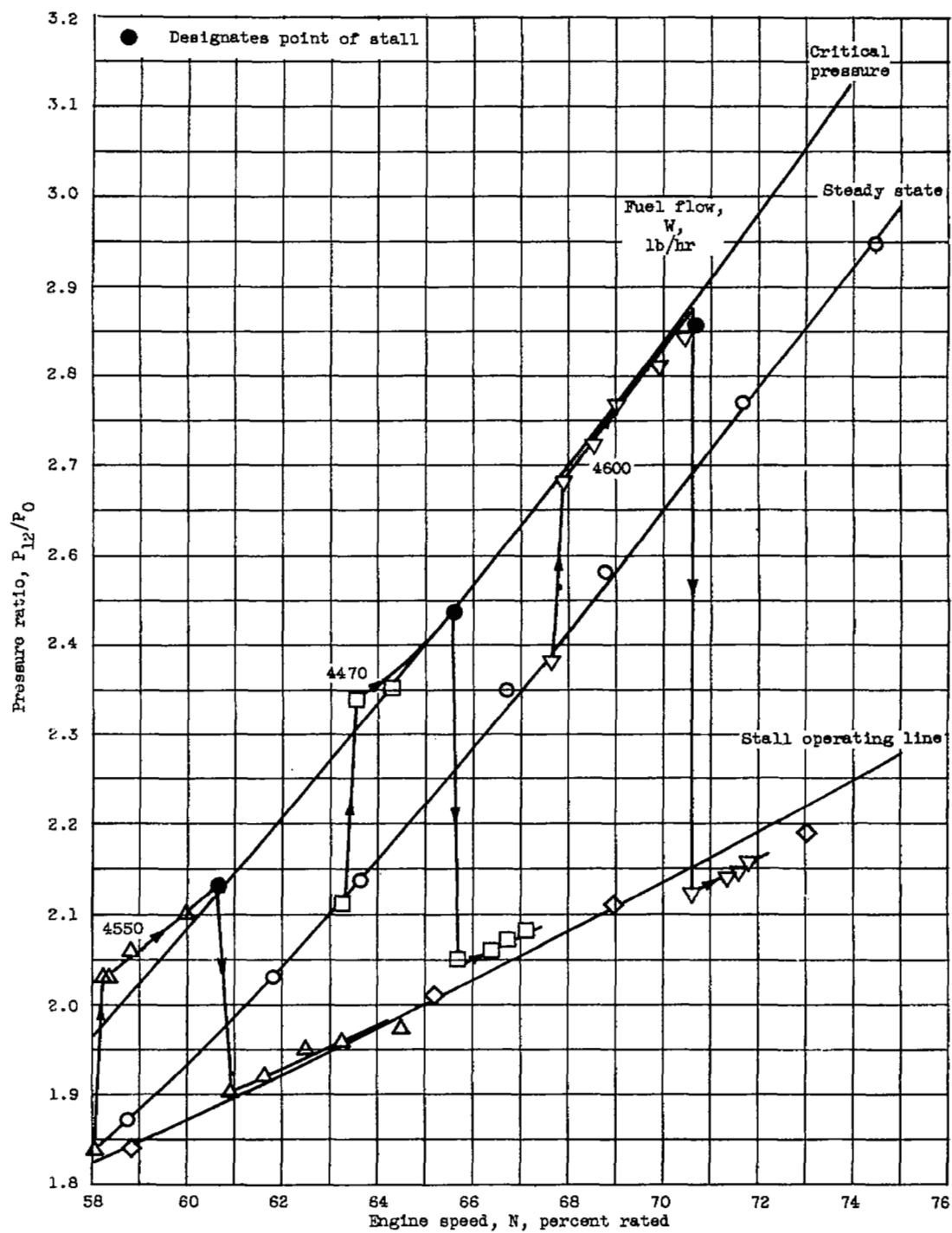
(b) Pressure loss during stall and surge. Engine speed, 53 percent rated.

Figure 11. - Concluded. Pressure ratio developed during acceleration.



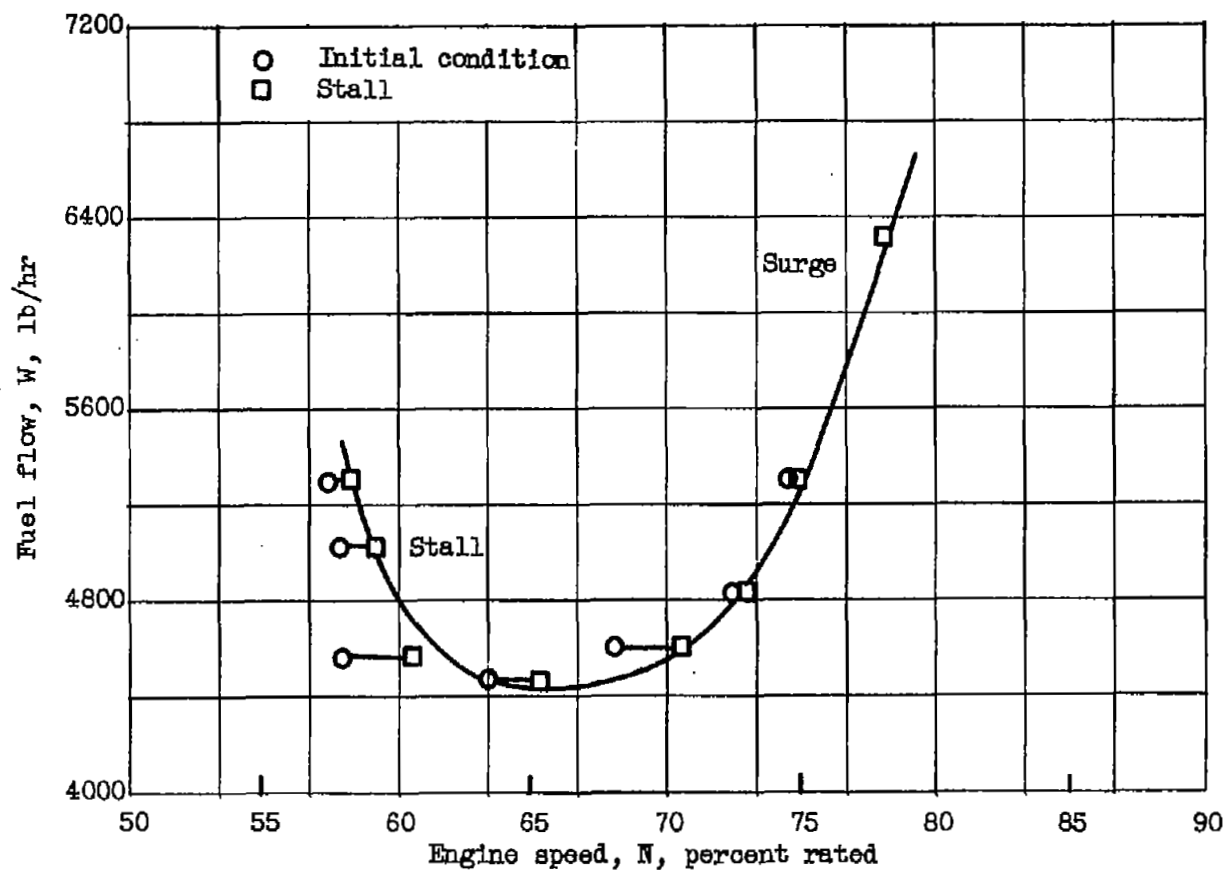
(a) Fuel flow increases at same initial speed.

Figure 12. - History of compressor-discharge total-pressure ratio during acceleration in vicinity of stall.



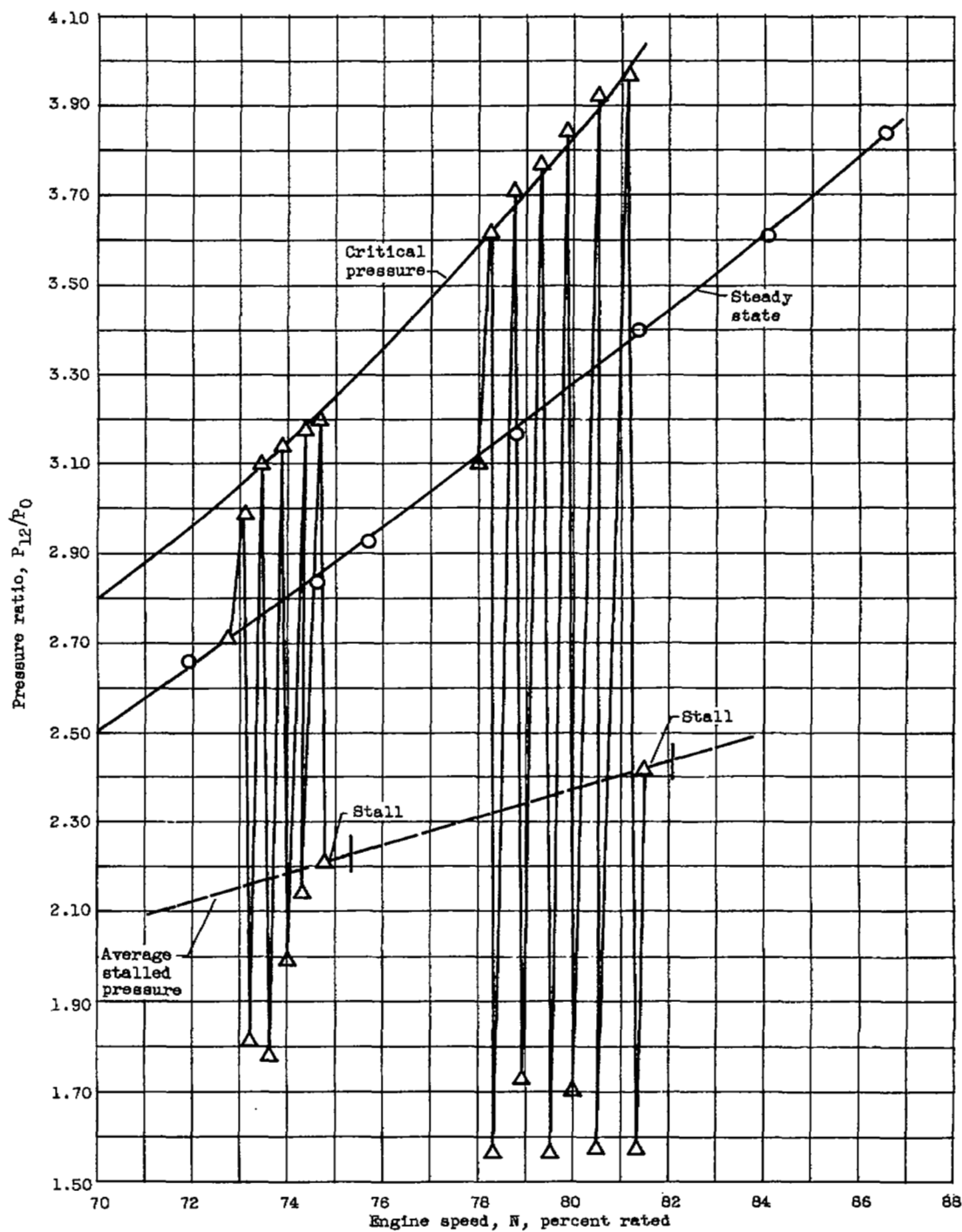
(b) Fuel flow increases at different initial speeds.

Figure 12. - Continued. History of compressor-discharge total-pressure ratio during acceleration in vicinity of stall.



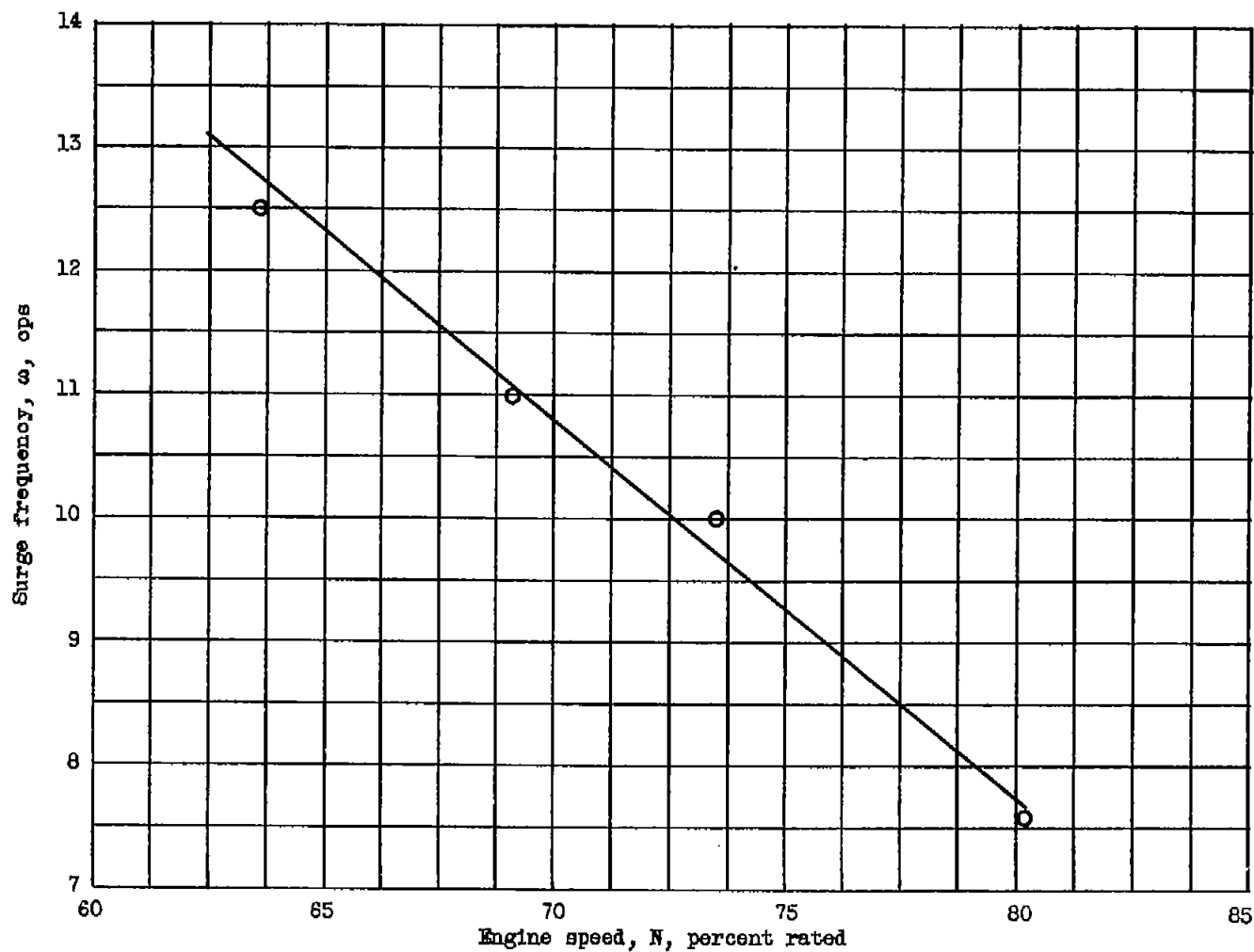
(c) Maximum fuel flow schedule.

Figure 12. - Concluded. History of compressor-discharge total-pressure ratio during acceleration in vicinity of stall.



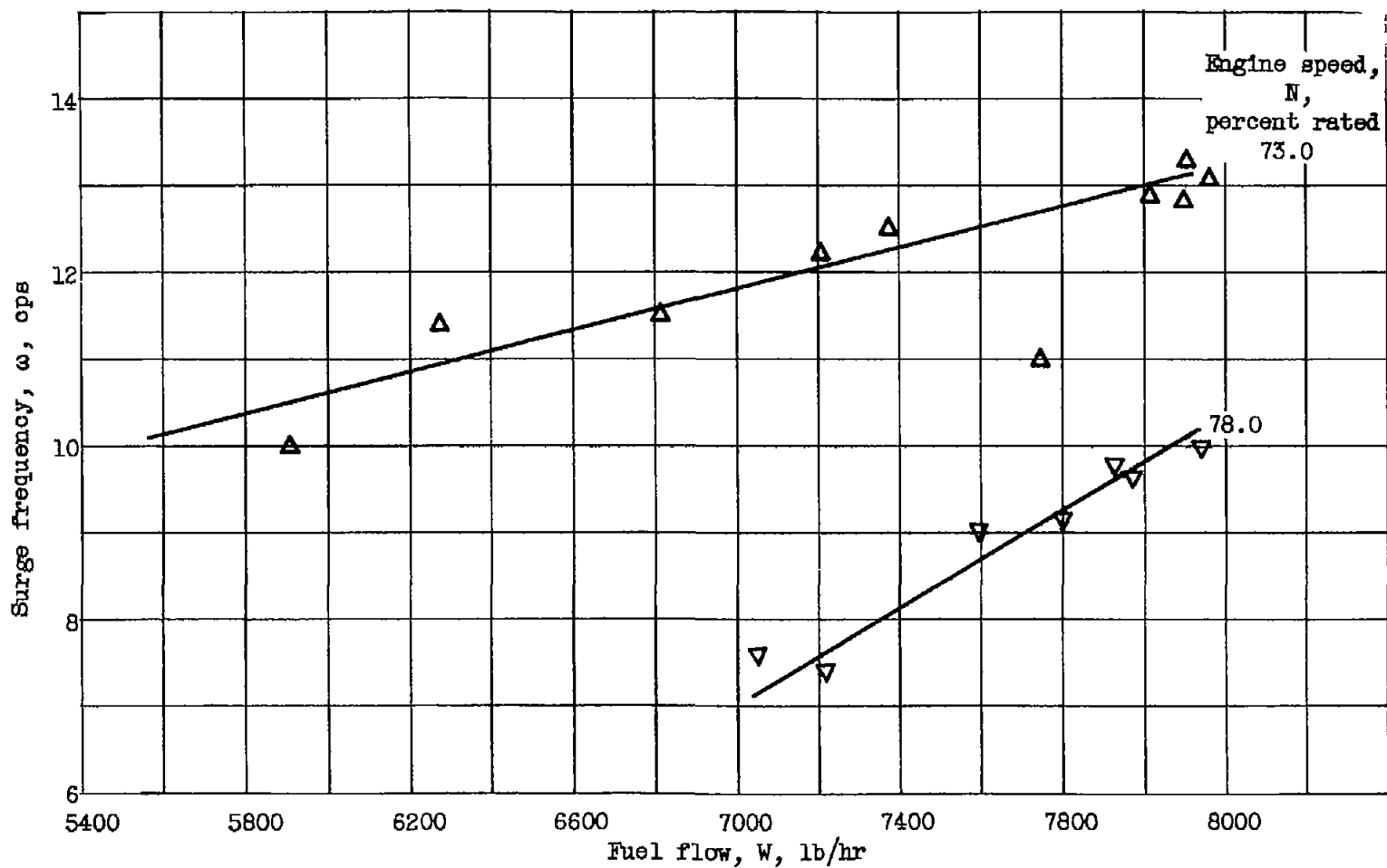
(a) Accelerations starting from two initial speeds (72.8 and 78.0 percent rated).

Figure 13. - Behavior of compressor total-pressure ratio during acceleration in vicinity of surge.



(b) Effect of initial engine speed on surge frequency.

Figure 13. - Continued. Behavior of compressor total-pressure ratio during acceleration in vicinity of surge.



(c) Effect of fuel flow on surge frequency.

Figure 13. - Concluded. Behavior of compressor total-pressure ratio during acceleration in vicinity of surge.

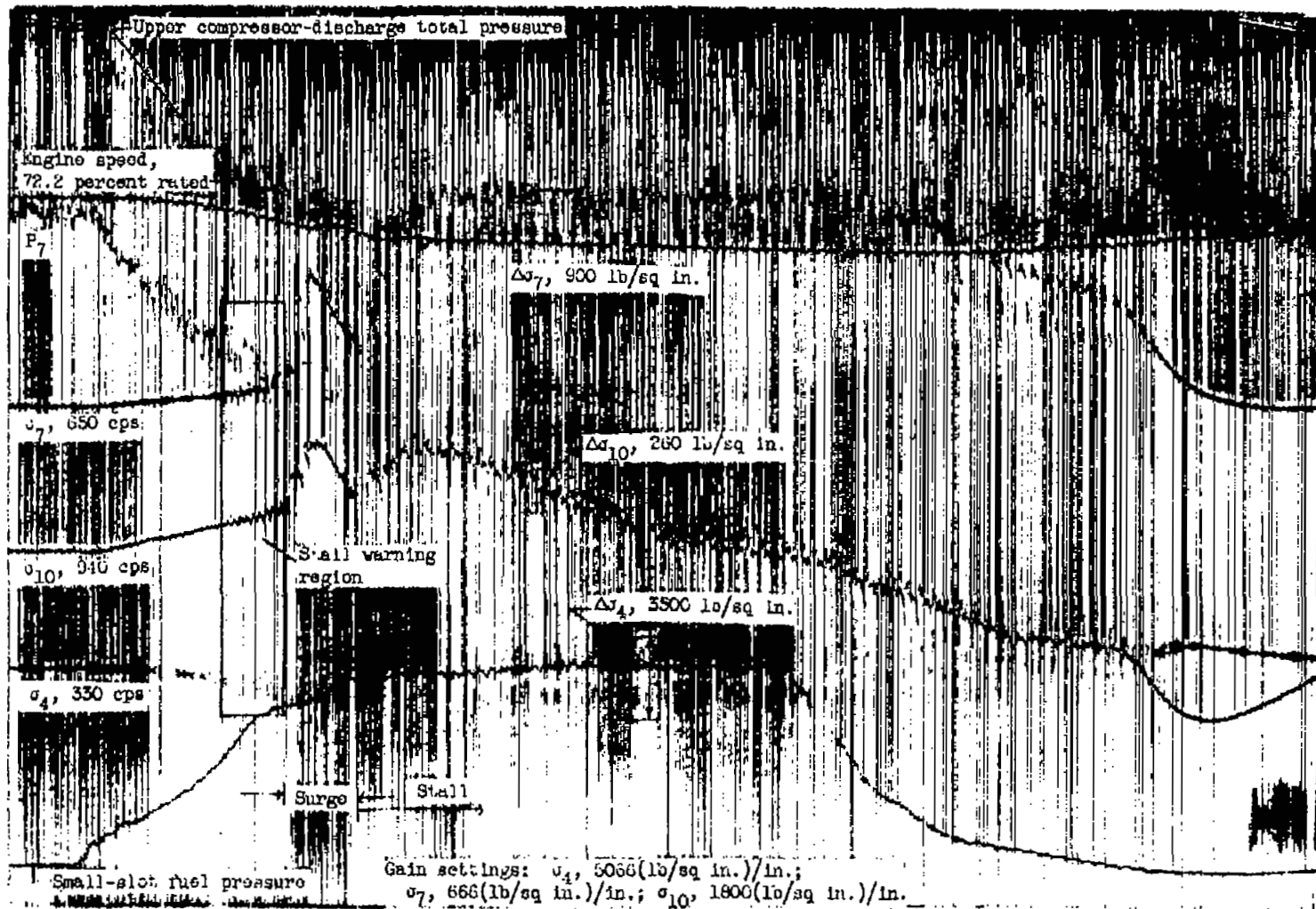
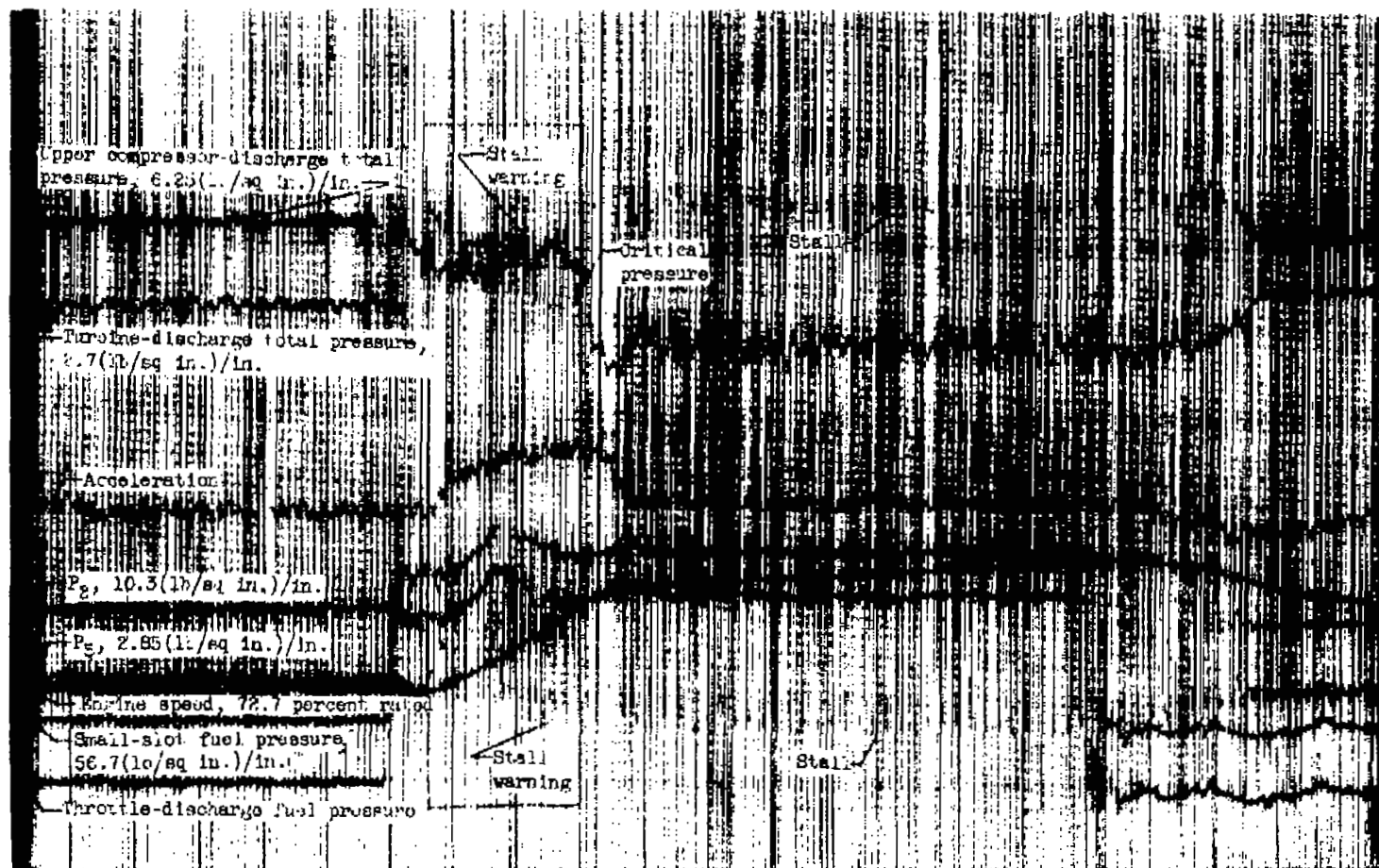
(a) Blade stresses σ .

Figure 14. - Parameters useful as prestall warnings.



(b) Pressure responses P to step changes in fuel flow.

Figure 14. - Continued. Parameters useful as prestall warnings.

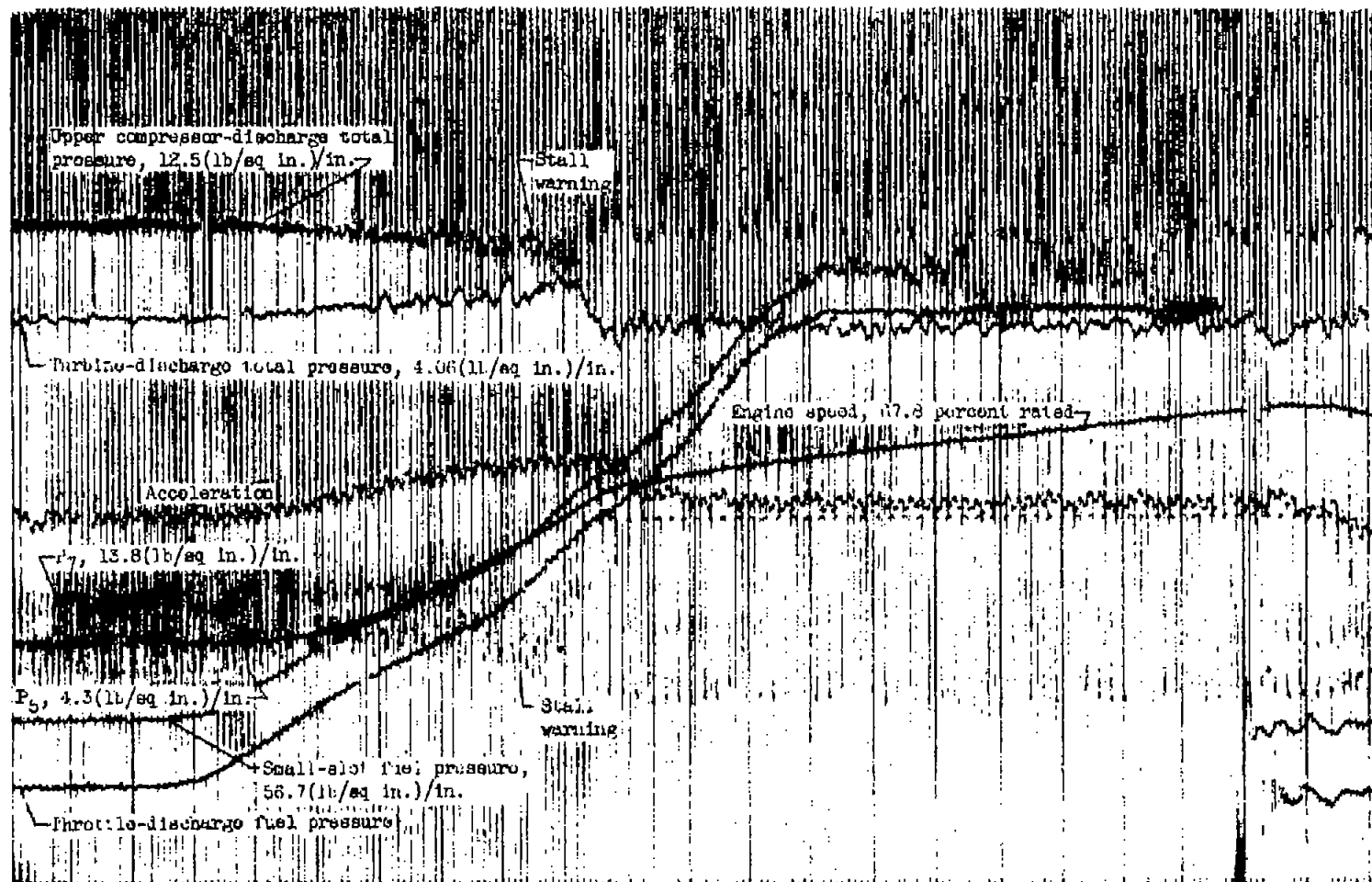
(c) Pressure responses P to ramp changes in fuel flow.

Figure 14. - Concluded. Parameters useful as prestall warnings.

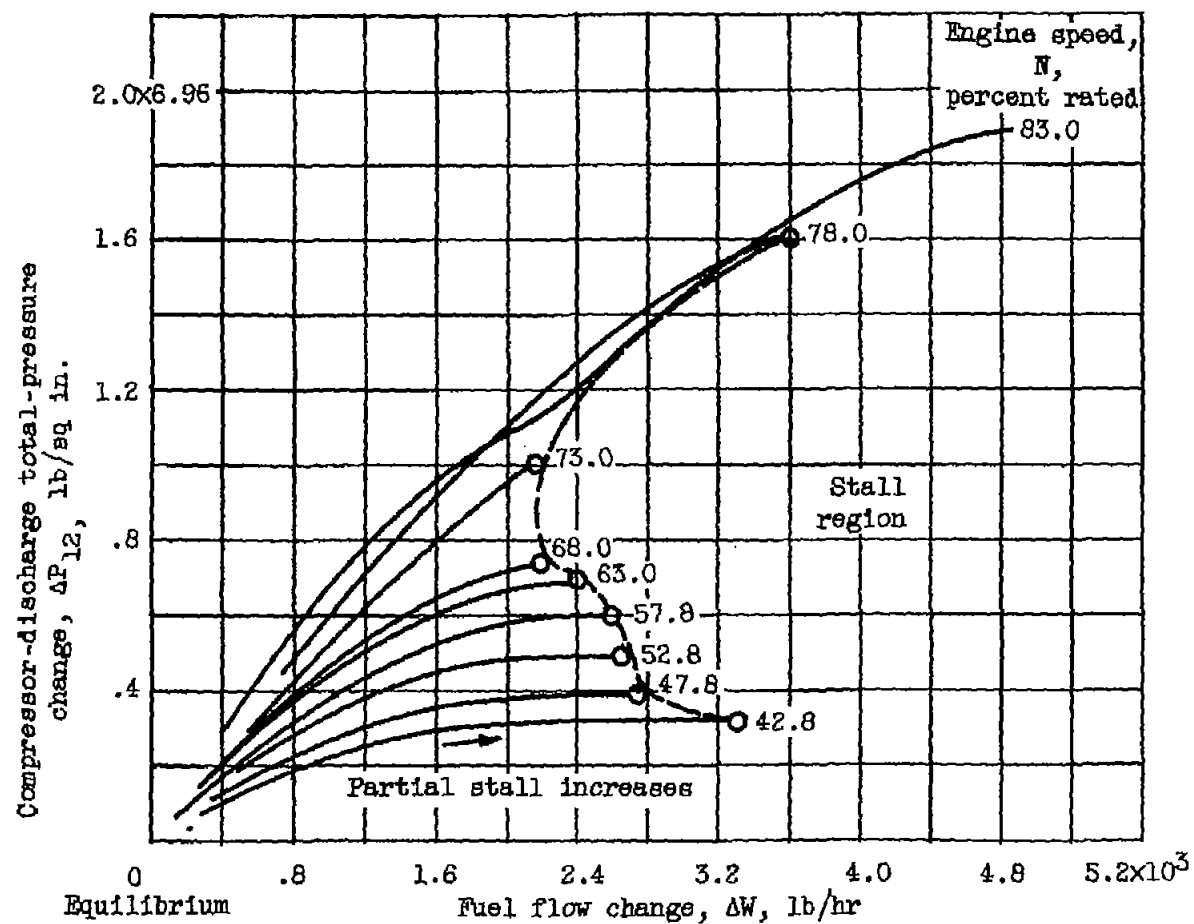
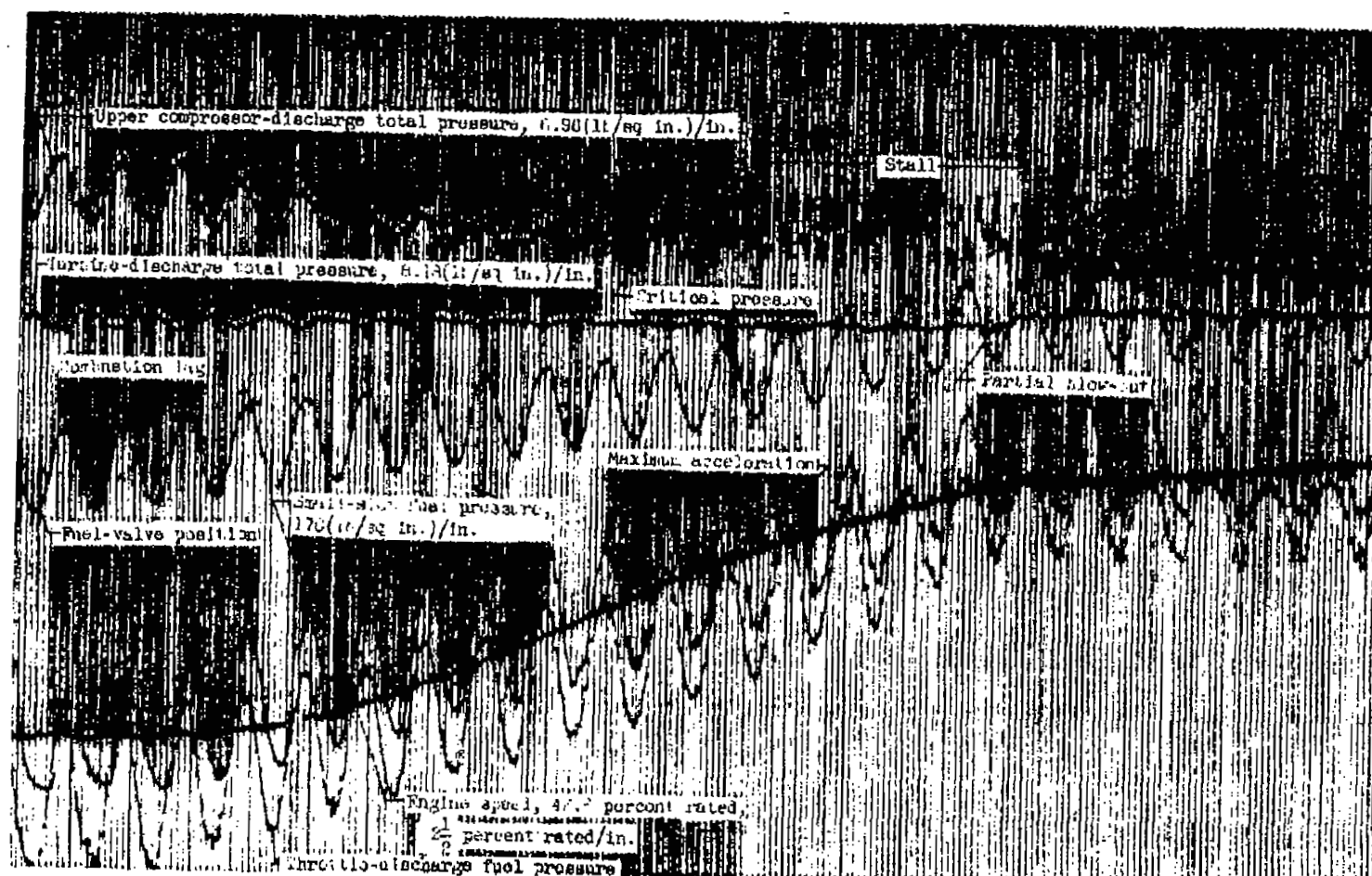
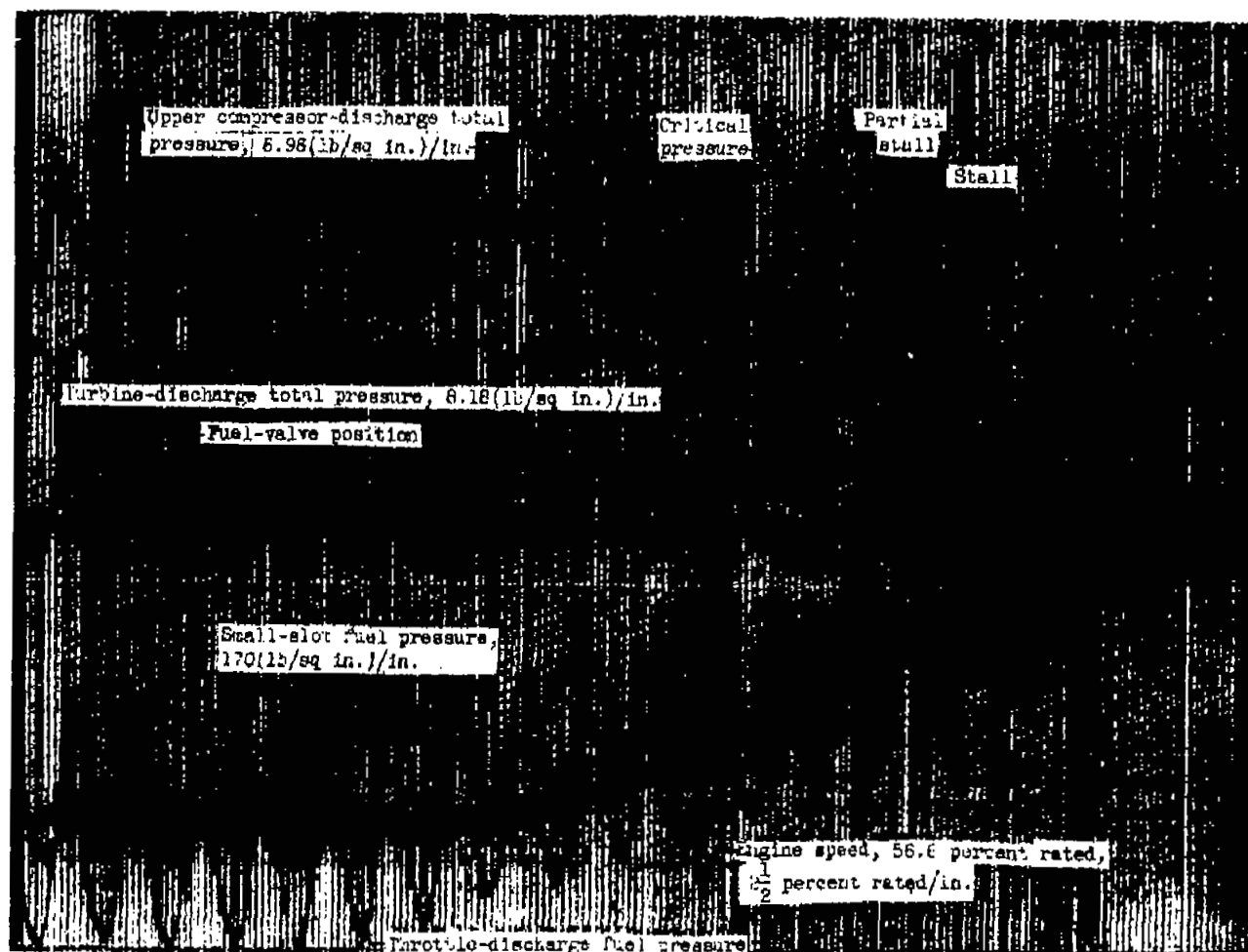


Figure 15. - Saturation effect in compressor pressure response to fuel increases.



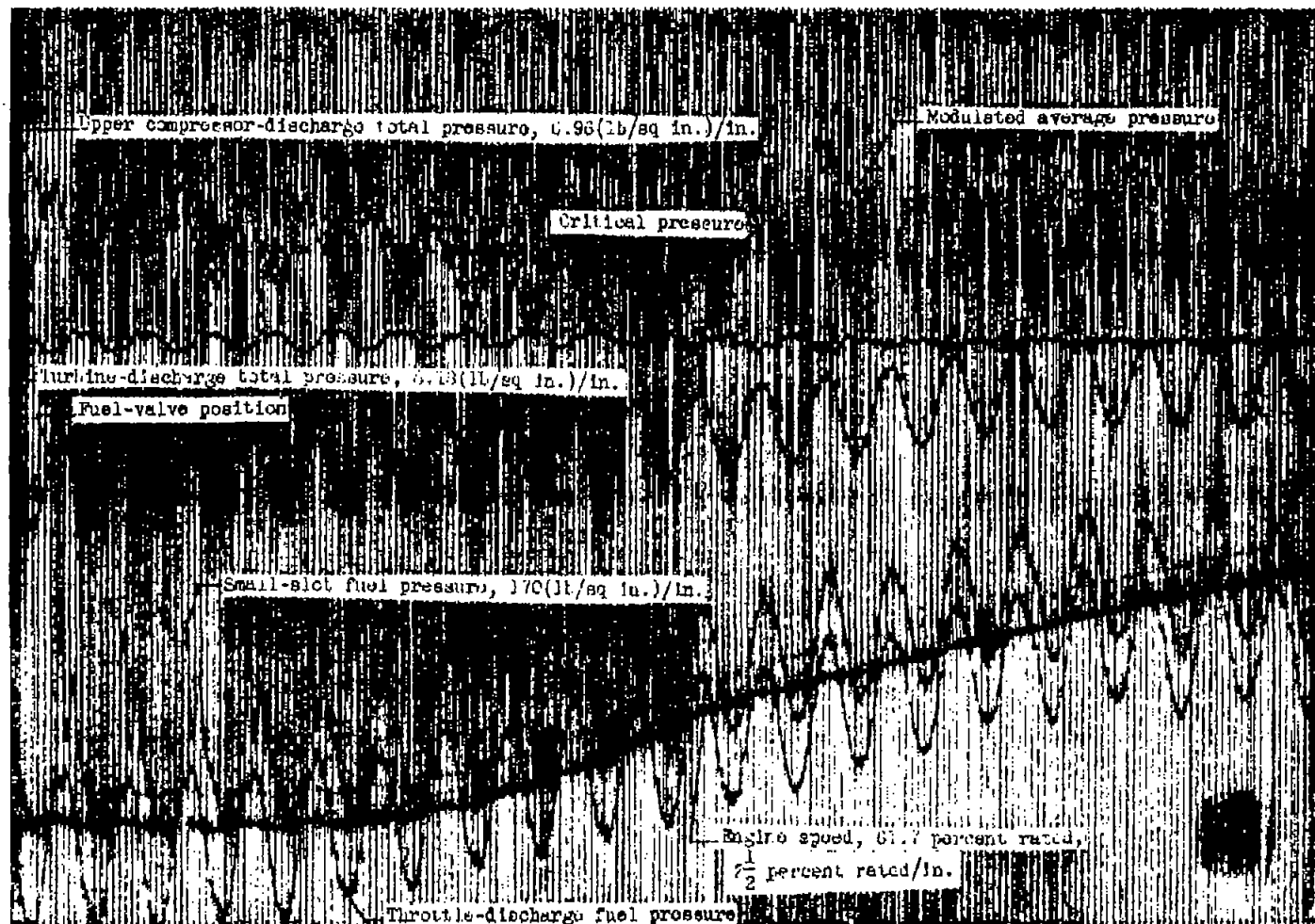
(a) Initial engine speed N , 46.6 percent rated

Figure 16. - Engine responses to simulated continuous-test-signal inputs for optimizing controls.



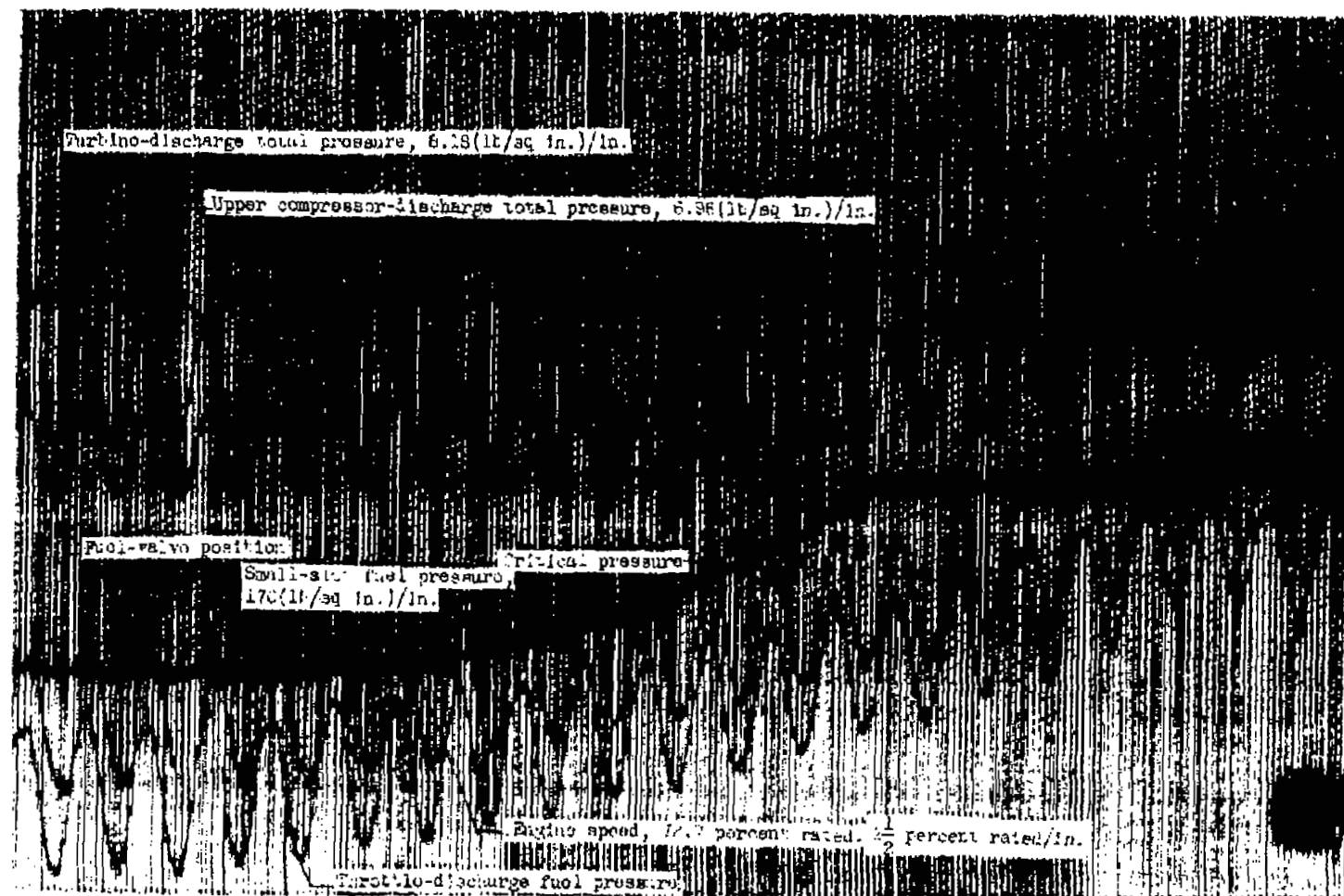
(b) Initial engine speed N , 56.6 percent rated.

Figure 16. - Continued. Engine responses to simulated continuous-test-signal inputs for optimizing controls.



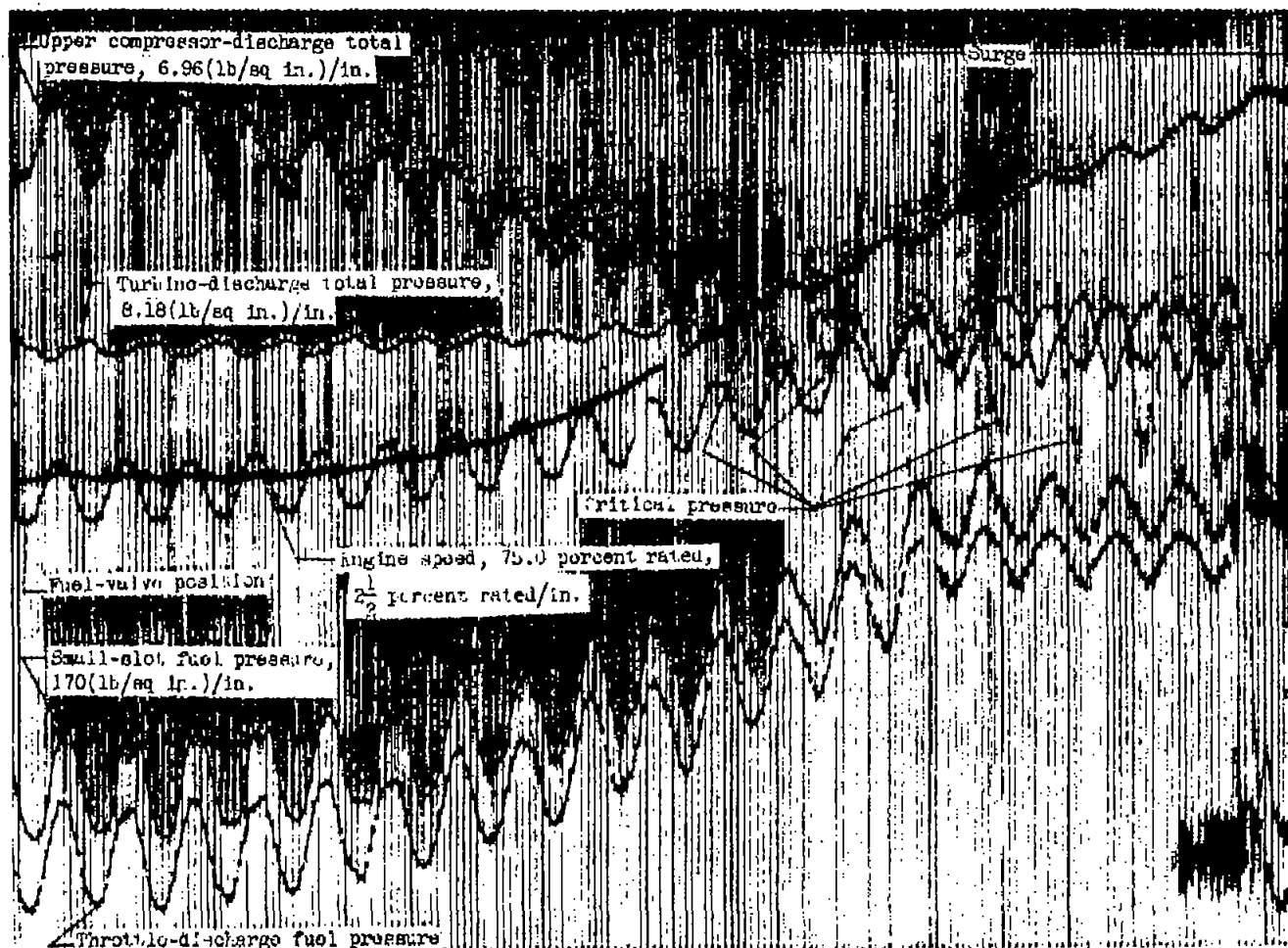
(c) Initial engine speed N_i 61.7 percent rated.

Figure 18. - Continued. Engine responses to simulated continuous-test-signal inputs for optimizing controls.



(d) Initial engine speed N , 72.7 percent rated.

Figure 16. - Continued. Engine responses to simulated continuous-test-signal inputs for optimizing controls.



(e) Initial engine speed N , 75.0 percent rated.

Figure 16. - Concluded. Engine responses to simulated continuous-test-signal inputs for optimizing controls

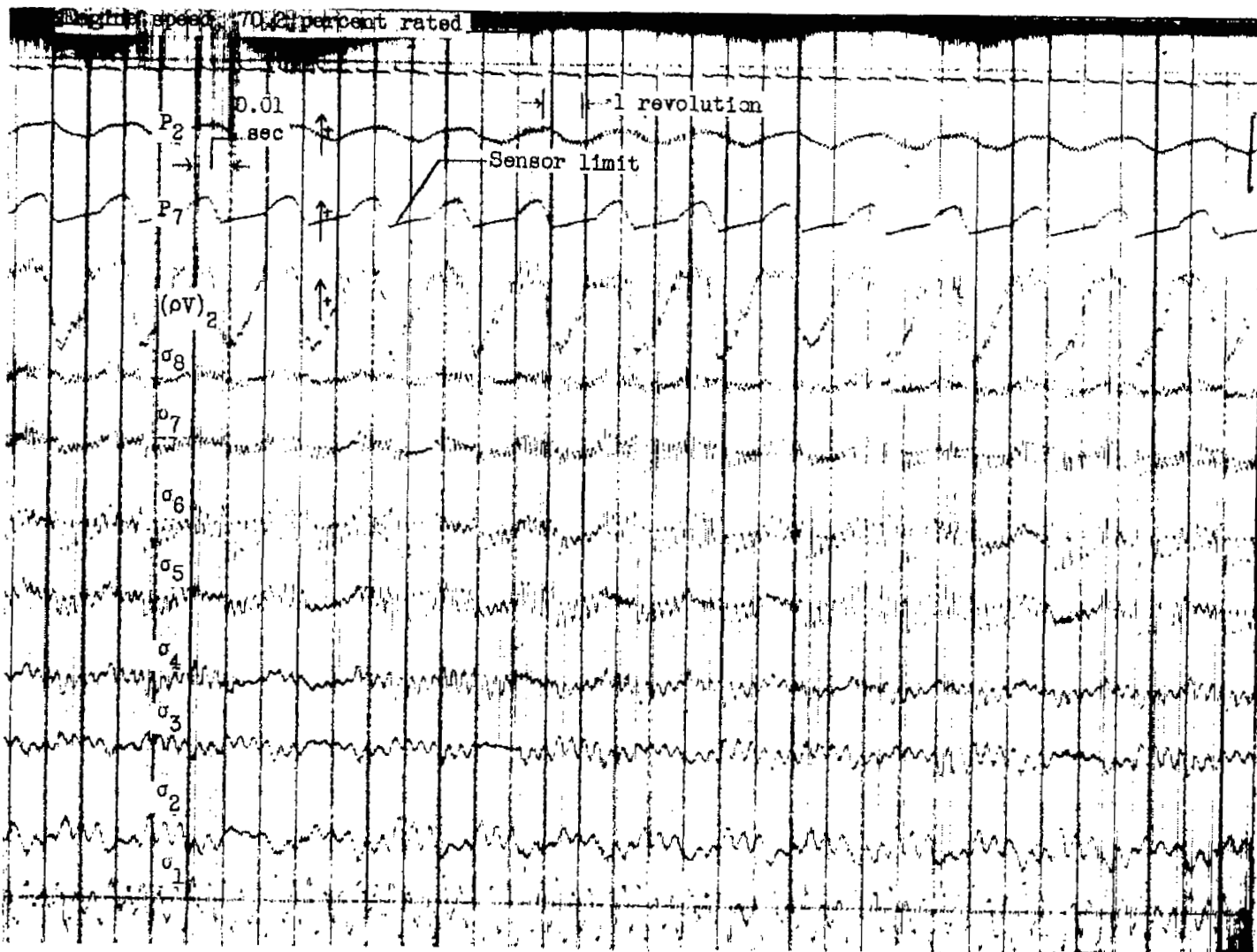
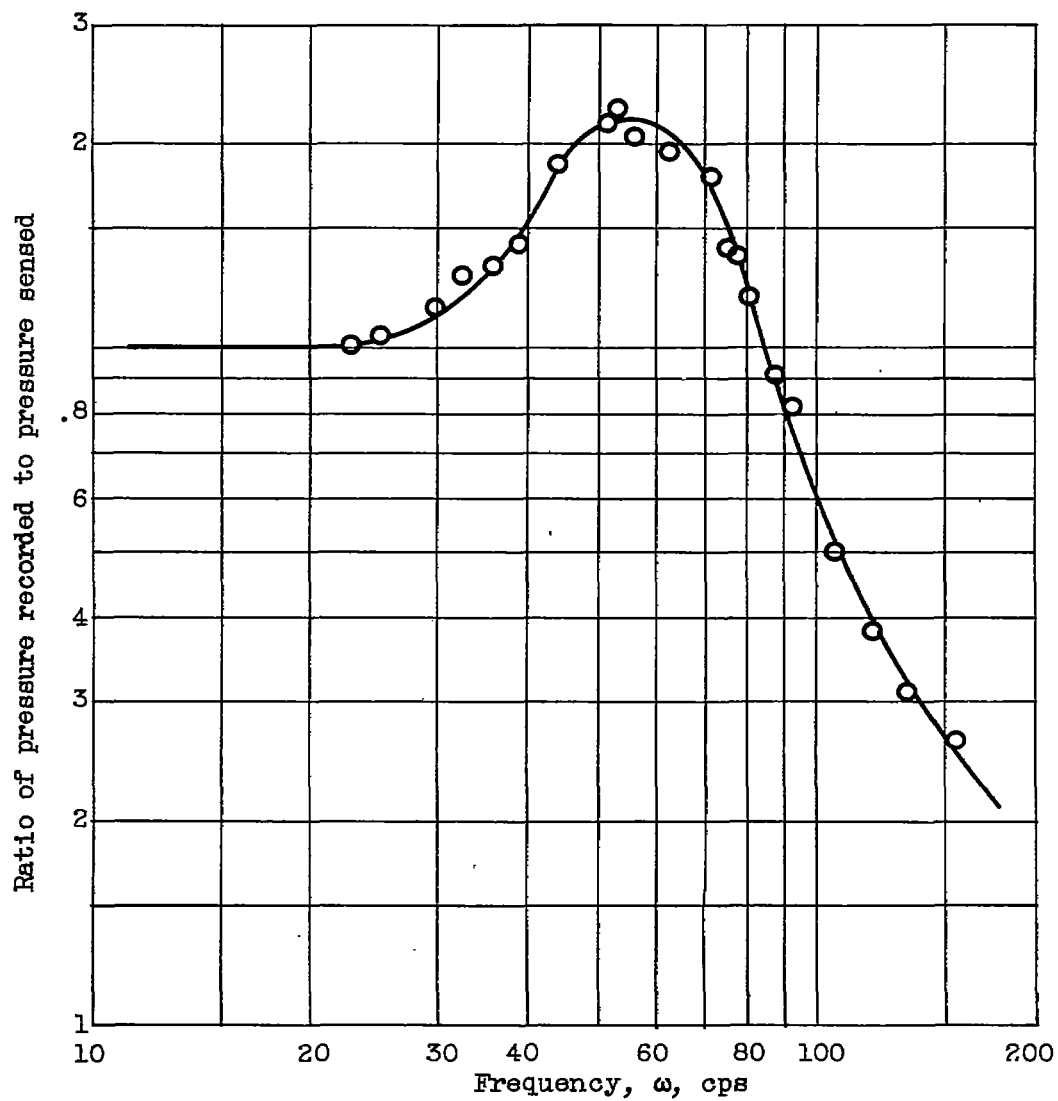
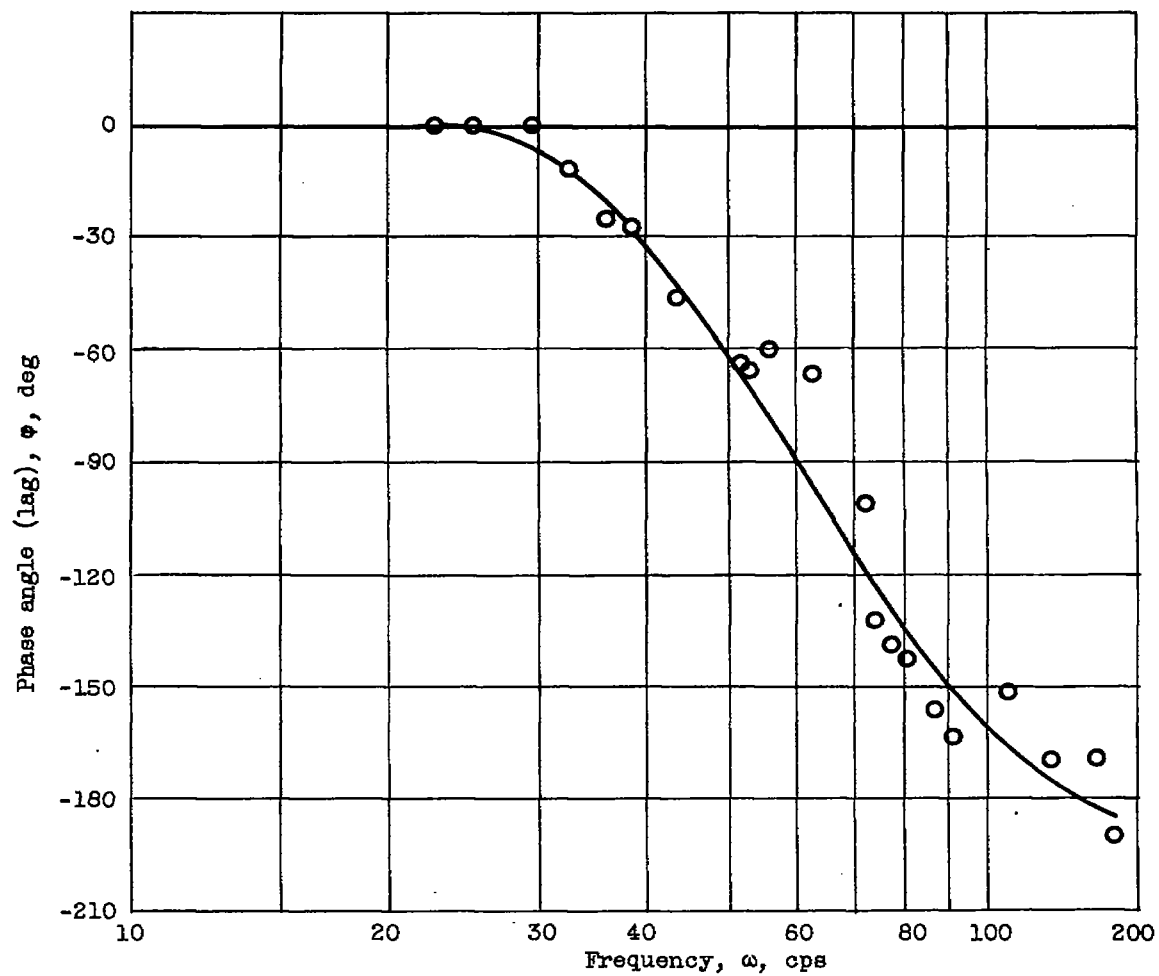


Figure 17. - Comparison of total pressures P with mass flow $(pV)_2$ during stalled turbojet-engine behavior.



(a) Amplitude.

Figure 18. - Frequency response of typical pressure probe.



(b) Phase angle.

Figure 18. - Concluded. Frequency response of typical pressure probe.

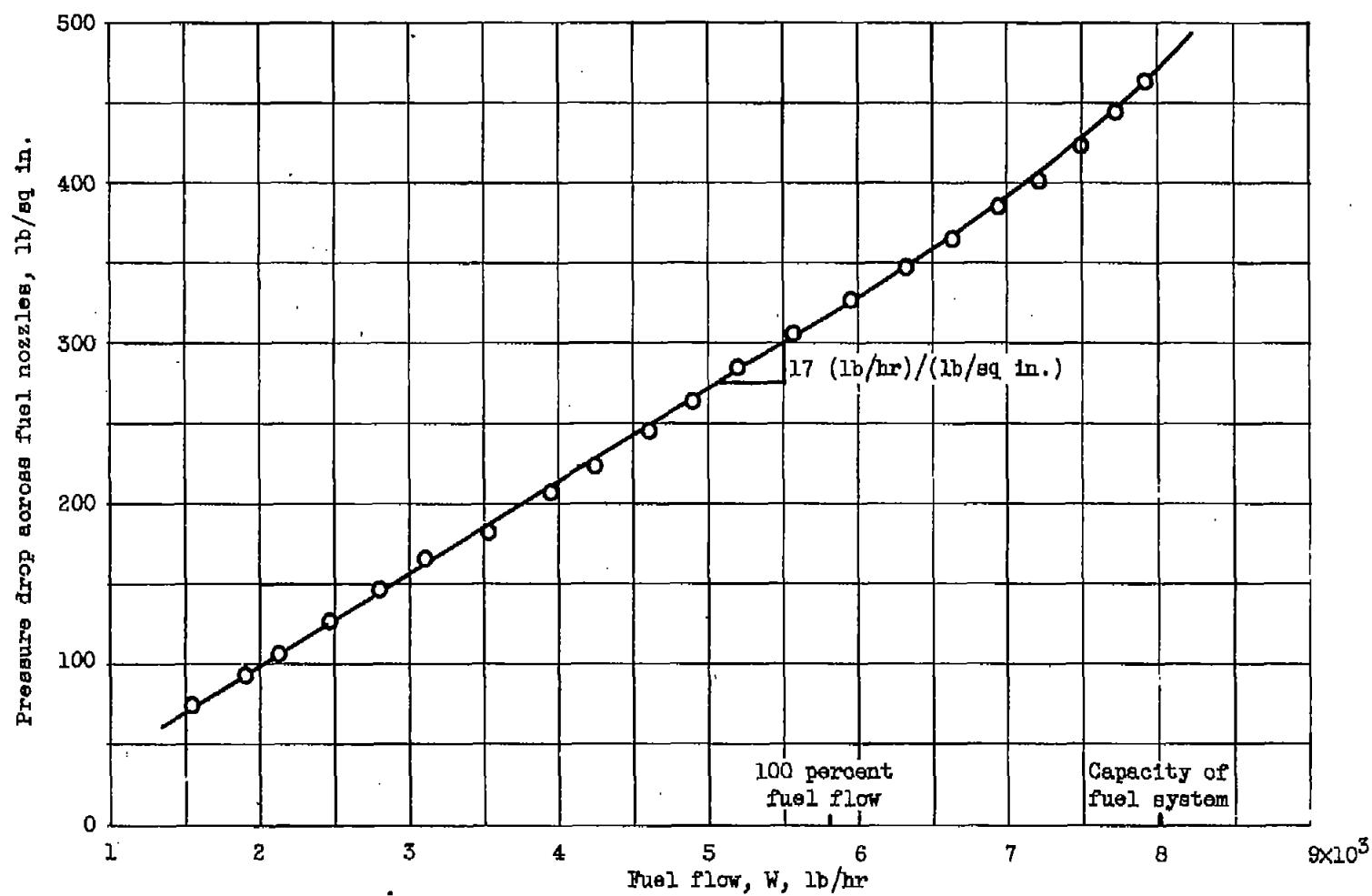


Figure 19. - Relation between actual fuel flow and pressure drop across fuel nozzles.

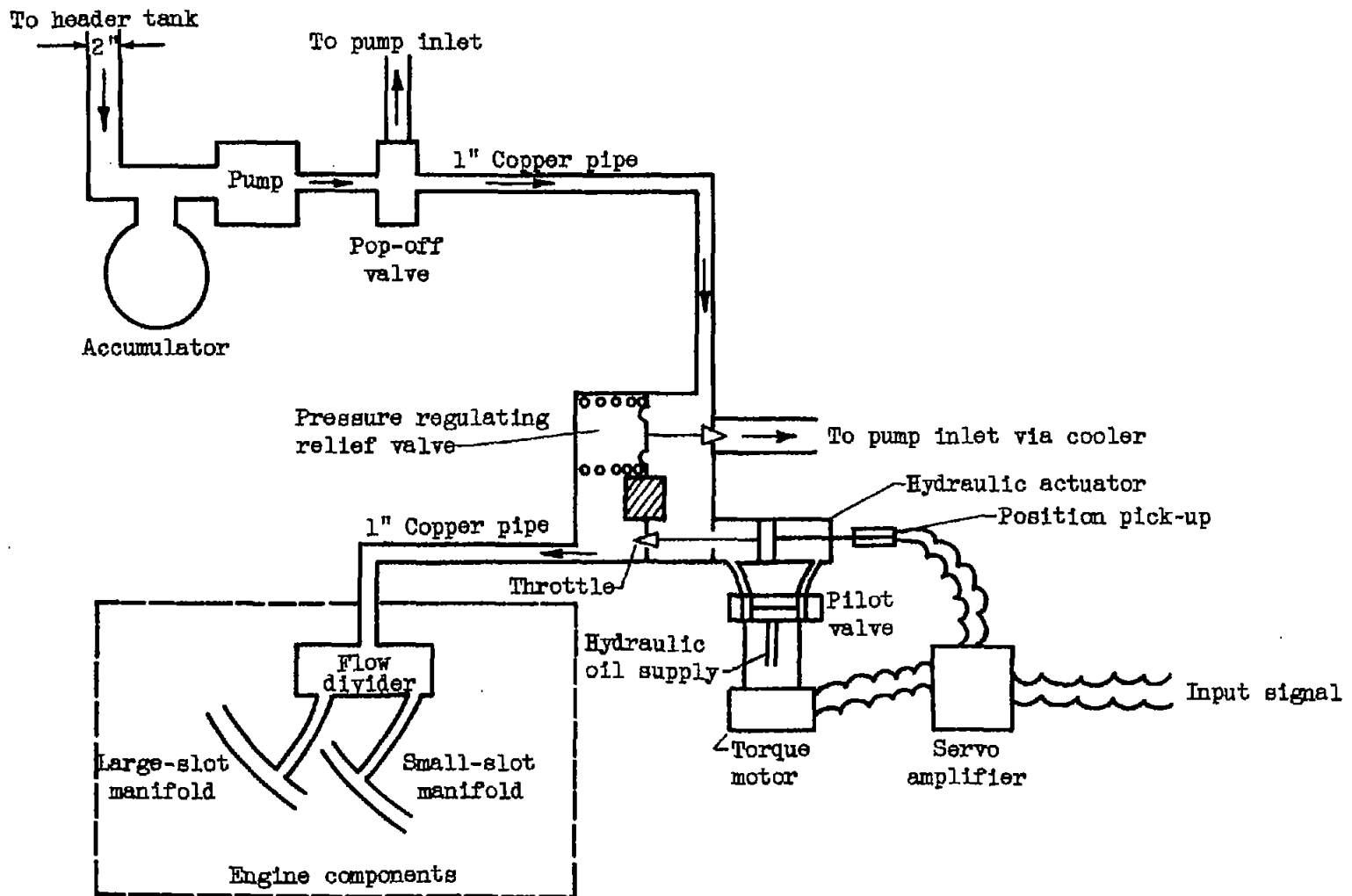



Figure 20. - Schematic diagram of fuel system.

[REDACTED]

NASA Technical Library



3 1176 01435 7348

1
3

7
V

1
1

[REDACTED]